

**CARBON MOLECULAR SIEVE MEMBRANES FOR  
OXYGEN SEPARATION**

BY  
**TANVEERULLA HUSSAIN SYED**

A Thesis Presented to the  
DEANSHIP OF GRADUATE STUDIES

**KING FAHD UNIVERSITY OF PETROLEUM & MINERALS**

DHAHRAN, SAUDI ARABIA

In Partial Fulfillment of the  
Requirements for the Degree of

**MASTER OF SCIENCE**

In  
**MECHANICAL ENGINEERING**

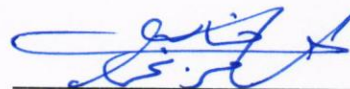
April 2016

KING FAHD UNIVERSITY OF PETROLEUM & MINERALS

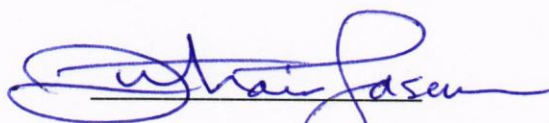
DHAHRAN- 31261, SAUDI ARABIA

**DEANSHIP OF GRADUATE STUDIES**

This thesis, written by **TANVEERULLA HUSSAIN SYED** under the direction of his thesis advisor and approved by his thesis committee, has been presented and accepted by the Dean of Graduate Studies, in partial fulfillment of the requirements for the degree of **MASTER OF SCIENCE IN MECHANICAL ENGINEERING.**



Dr. Khaled Mezghani  
(Advisor)



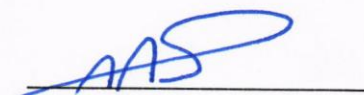
Dr. Zuhair M. A. Gasem  
Department Chairman



Dr. Abdul Samad Mohammed  
(Member)



Dr. Salam A. Zummo  
Dean of Graduate Studies



Dr. Ahmad A. Sorour  
(Member)

12/7/16  
Date

© Tanveerulla Hussain Syed

2016

## *Dedication*

I dedicate this work to my parents for their love and support during my studies abroad.

## **ACKNOWLEDGMENTS**

I would like to thank Allah (SWT) for his guidance and support.

I thank King Fahd University of Petroleum and Minerals for giving this opportunity to complete my graduate study. My admission to KFUPM was greatly assisted by a dear friend, Mr. Mohammed Haseebuddin, and I would like to express my deepest thanks to him.

My sincere gratitude and thanks to my thesis advisor Dr. Khaled Mezghani for introducing me to this area of research – Polymer membrane technology. His guidance and support helped me in the duration of this research and thesis write-up. I am very grateful to have him as my thesis advisor and mentor.

I thank my committee members, Dr. Abdul Samad Mohammed and Dr. Ahmad A. Sorour for their assistance in my research. I would like to thank the funding from KACST-TIC. I thank my project members, Mr. Sarfaraz Ahmed, Mr. Ameer Hamza and Mr. Khaja Ameruddin for their company. I thank the lab engineers Mr. Abdul Lathif and Mr. Sadaqat for their assistance with the instruments.

I thank my roommate Abdul Rahman Aliyu and friends Rehan Khan, Jazeem Jaleel, Annas Bin Ali, Junaid Ahmed, Irfan Somrow and others who made my stay in KFUPM a memorable experience. I thank my seniors Abdurrahman, Zabiullah, Yousuf, Riaz, Fasi and Abdul Azeem for their support. Finally, I would like to thank my family for their prayers and well wishes during my stay abroad.

# TABLE OF CONTENTS

ACKNOWLEDGMENTS.....	V
TABLE OF CONTENTS.....	VI
LIST OF TABLES.....	IX
LIST OF FIGURES.....	X
LIST OF ABBREVIATIONS.....	XII
ABSTRACT.....	XV
ملخص الرسالة.....	XVII
<b>CHAPTER 1 INTRODUCTION.....</b>	<b>1</b>
1.1 Gas Separation .....	1
1.2 Conventional Gas Separation Technologies .....	3
1.2.1 Sorption Processes .....	3
1.2.2 Cryogenic Distillation.....	4
1.3 Membranes For Gas Separation .....	4
1.3.1 Advantages Of Choosing Membranes Over Other Gas Separation Technologies .....	4
1.3.2 Membranes .....	5
1.4 Carbon Molecular Sieves .....	8
1.5 Oxygen Separation .....	11
1.6 Objectives.....	15
<b>CHAPTER 2 LITERATURE REVIEW .....</b>	<b>16</b>
2.1 GAS TRANSPORT IN MEMBRANES .....	16

2.2	GAS TRANSPORT MECHANISMS .....	17
2.2.1	CONVECTIVE FLOW .....	17
2.2.2	KNUDSEN DIFFUSION .....	18
2.2.3	MOLECULAR SIEVING EFFECT .....	19
2.2.4	THE SOLUTION-DIFFUSION MODEL .....	20
2.3	SELECTION OF PRECURSOR .....	23
2.4	PRETREATMENT.....	24
2.5	PYROLYSIS .....	25
2.6	EFFECT OF PYROLYSIS VARIABLES .....	27
2.6.1	Effect of Pyrolysis Temperature .....	27
2.6.2	Effect of Vacuum Atmosphere .....	27
2.6.3	Effect of Inert Gas flowrate .....	28
2.6.4	Effect of Soak Time .....	29
2.6.5	Effect of Heating Rate .....	29
2.7	POST TREATMENT .....	30
<b>CHAPTER 3 EXPERIMENTAL.....</b>		<b>31</b>
3.1	POLYMER PRECURSOR.....	31
3.2	PRE TREATMENT OF THE POLYMER .....	32
3.3	CARBONIZATION .....	35
3.4	PERMEATION SET-UP.....	36
3.5	PERMEATION MEASUREMENT.....	38
3.5.1	PERMEABILITY (P).....	39
3.5.2	DIFFUSIVITY (D) .....	40
3.5.3	SOLUBILITY (S) .....	40

3.5.4	SELECTIVITY ( $\alpha$ ).....	41
3.6	CHARACTERIZATION METHODS .....	41
3.6.1	Thermo Gravimetric Analysis.....	41
3.6.2	Scanning Electron Microscopy .....	42
3.6.3	X-Ray Diffraction .....	42
3.6.4	Fourier Transforms Infrared Spectroscopy.....	42
<b>CHAPTER 4 RESULTS AND DISCUSSIONS.....</b>		<b>43</b>
4.1	TIME LAG ANALYSIS.....	43
4.2	GAS TRANSPORT PROPERTIES.....	44
4.2.1	CMS derived from different Kapton Films.....	44
4.2.2	Varying pyrolysis parameters .....	47
4.2.3	Pre Treated Samples.....	51
4.2.4	Post Heat Treated CMS Samples.....	55
4.2.5	Optimized Samples.....	57
<b>CHAPTER 5 CONCLUSIONS .....</b>		<b>67</b>
<b>CHAPTER 6 RECOMMENDATIONS FOR FUTURE WORK.....</b>		<b>69</b>
<b>REFERENCES.....</b>		<b>72</b>
<b>VITAE.....</b>		<b>87</b>

## LIST OF TABLES

Table 1: Commercial Membranes for Oxygen Separation[44].....	14
Table 2: Various Polymers, Their Pyrolysis Conditions and Permeation Properties. ....	26
Table 3: Sample Names and Their Description .....	33
Table 4: Permeation Properties of CMSM Derived from Different Kapton Films .....	44
Table 5: Permeation Properties of CMSM Derived by Changing Pyrolysis Environment .....	48
Table 6: Permeation Properties of CMSM Derived by Changing Pyrolysis Temperature	50
Table 7: Permeation Properties of CMSM Derived from Preheated Kapton Films .....	51
Table 8: Permeation Properties of CMSM Derived from Chemically Treated Kapton Film .....	53
Table 9: Permeation Properties of Post Heat Treated CMS Samples.....	55
Table 10: Permeation Properties of Kapton Before and After Pyrolysis with Various Pre and Post Treatments.....	58

## LIST OF FIGURES

Figure 1: Gas Pairs Separated Using Membranes and Their Applications [3] .....	1
Figure 2: Important Milestones Achieved in Gas Separation .....	2
Figure 3: Schematic of Membrane Separation.....	6
Figure 4: Robeson Upper Bound .....	9
Figure 5: Illustration of Degrees of Freedom of O <sub>2</sub> , N <sub>2</sub> Molecules in Slit-Shaped Pore in CMS Membrane.....	10
Figure 6: Steps Involved in the Successful Fabrication of CMS[36] .....	11
Figure 7: Molecular Sizes of N <sub>2</sub> and O <sub>2</sub> .....	12
Figure 8: Single and Two-Stage Oxygen Separation Process. ....	13
Figure 9: Oxygen Separation Performance of Commercial Membranes. ....	14
Figure 10: Gas Permeation Mechanisms. ....	17
Figure 11: Illustration of Membrane.....	20
Figure 12: Chemical Structure of (a) Kapton (b) NMP .....	31
Figure 13: Polymer Precursors Prior to Pyrolysis.....	32
Figure 14: Schematic of Pyrolysis Setup.....	35
Figure 15: Polymer Precursors After Pyrolysis .....	36
Figure 16: Schematic of Permeation Setup.....	37
Figure 17: Pressure vs Time Response of an Ideal Time Lag Experiment.....	39
Figure 18: Pressure vs Time Plots for Oxygen and Nitrogen Permeation.....	43
Figure 19: FTIR of Different Kapton Films .....	45
Figure 20: Permeation Properties of CMSM Derived From Different Kapton Films. ..	46

Figure 21: TGA Thermograms of Kapton® polyimide .....	47
Figure 22: Permeation Properties of CMSM Derived by Varying Pyrolysis Atmosphere .....	49
Figure 23: Permeation Properties of CMSM Derived by Changing Pyrolysis Temperature .....	50
Figure 24: Permeation Properties of CMSM Membranes Derived from Preheated Kapton Films.....	52
Figure 25: Permeation Properties of CMSM Derived from Chemically Pretreated Samples.....	54
Figure 26: Permeation Properties of Post Heat Treated CMSM.....	56
Figure 27: Oxygen Doping During the Oxidation of CMS membrane. ....	56
Figure 28: FTIR of Raw and Pretreated Kapton Films.....	60
Figure 29: XRD Spectra of Kapton .....	62
Figure 30: Atomic Structure of (a) Perfect Graphite (b) Turbo Static graphite .....	63
Figure 31: Surface Topologies of CMS membranes: (a) CMS; (b) CMS-HT-AP; (c) CMS-HT-BP; (d) CMS-NMP-CP; (e) CMS-NMP-IWT .....	64
Figure 32: Representation of Permeation Properties on Robeson's Plot .....	65

## LIST OF ABBREVIATIONS

<b>CA</b>	:	Cellulose Acetate
<b>CMS</b>	:	Carbon Molecular Sieves
<b>CVD</b>	:	Chemical Vapor Deposition
<b>DMF</b>	:	Di-Methyl Formamide
<b>DSC</b>	:	Differential Scanning Calorimetry
<b>EPDM</b>	:	Ethylene Propylene Diene Monomer
<b>FTIR</b>	:	Fourier Transform Infrared
<b>HCl</b>	:	Hydro Chloric acid
<b>HDPE</b>	:	High density poly ethylene
<b>HF</b>	:	Hydro Fluoric acid
<b>HP</b>	:	High Permeability
<b>LDPE</b>	:	Low density poly ethylene
<b>LP</b>	:	Low Permeability
<b>MOF</b>	:	Metal Organic Framework
<b>MP</b>	:	Medium Permeability

<b>NH<sub>4</sub>Cl</b>	:	Ammonium Chloride
<b>NMP</b>	:	N-Methyl Pyrrolidone
<b>OEA</b>	:	Oxygen Enriched Air
<b>PA</b>	:	Polyamides
<b>PAN</b>	:	Poly Acrylo Nitrile
<b>PDMS</b>	:	Poly (dimethyl siloxane)
<b>PES</b>	:	Poly Ether Sulfone
<b>PI</b>	:	Polyimide
<b>PPZ</b>	:	Poly Phospazene
<b>PSA</b>	:	Pressure Swing Absorption
<b>PSf</b>	:	Poly Sulfone
<b>SEM</b>	:	Scanning Electron Microscope
<b>STP</b>	:	Standard Temperature and Pressure
<b>TGA</b>	:	Thermo-Gravimetric Analysis
<b>TSA</b>	:	Temperature Swing Adsorption
<b>VLP</b>	:	Very Low Permeability
<b>VSA</b>	:	Vacuum Swing Adsorption

**XRD** : X-Ray Diffraction

**ZIF** : Zeolite Imidazolate Frameworks

**6FDA/BPDA-DAM** : 4,4'-(hexafluoroisopropylidene) diphthalic  
anhydride (6FDA)/3,3'- 4,4'-biphenyl  
tetracarboxylic acid dianhydride (BPDA) -  
2,4,6-trimethyl-1,3-phenylene diamine (DAM)

## **ABSTRACT**

Full Name : [Tanveerulla Hussain Syed]  
Thesis Title : [Carbon Molecular Sieve Membranes for Oxygen Separation]  
Major Field : [Mechanical Engineering]  
Date of Degree : [April 2016]

Over the past few decades, membranes have been used in various separation processes such as ultrafiltration, dialysis, desalination, reverse osmosis, dehumidification and gas separation. Polymer membranes are not able to fully exploit the needs of the gas separation because of their low chemical and thermal stabilities. A good alternative for this purpose is carbon molecular sieves (CMS). The CMS is reported to have good combination of permeability and selectivity of oxygen. These membranes are also capable of withstanding high temperatures and harsh chemical conditions due to their inert carbon matrix.

The aim of this study is to prepare efficient CMS membranes for oxygen separation and enhance the separation performance by various pre-treatments. The CMS membranes have been prepared via pyrolysis of a commercially available polyimide (Kapton). The pyrolysis parameters such as heating rate, soaking time, temperature, and atmosphere are adjusted in order to achieve an optimum permeability and selectivity of the membrane.

In this study, two types of pretreatments (oxidation and chemical) have been applied to the polymeric precursor, Kapton, prior to the pyrolysis step. Firstly, the Kapton membrane is pre-treated using N-Methyl Pyrrolidone (NMP). This chemical pre-

treatment improved the selectivity (up to 10.81) of the CMS membrane while retaining high permeability of 26 barrers. Secondly, the Kapton membrane has been subjected to heat treatment in an oxidative environment (air) at 350°C for one hour. This oxidation heat-treatment has improved the permeability up to 50 barrers. The membranes were characterized using Scanning electron microscope (SEM), Thermo gravimetric analyzer (TGA), Fourier transforms infrared spectroscopy (FTIR) and X-ray diffraction (XRD). It has been confirmed that these membranes exhibit molecular sieving properties in separating oxygen from nitrogen.

## ملخص الرسالة

الاسم الكامل : تنوير الله حسين سيد

عنوان الرسالة: أغشية الكربون المنخل الجزيئي لفصل الاوكسجين من الهواء

التخصص: الهندسة الميكانيكية

تاريخ الدرجة العلمية: ابريل 2016

على مدى العقود القليلة الماضية، استُخدمت الاغشية في كثير من عمليات الفصل المختلفة مثل الترشيح الفائق، غسيل الكلى، تحلية المياه، التناضح العكسي، التجفيف وفصل الغاز. ونظراً لعدم ثبات الاغشية البوليمرية كيميائياً وحرارياً، فإنها ليست قادرة على التلبية الكاملة لمتطلبات فصل الغازات. كبديل جيد لهذا الغرض سيتم تطوير أغشية غير عضوية مثل الكربون المناخل الجزيئي (carbon molecular sieves, CMS). هذه الأغشية جيدة بما لديها من مزيج صفات النفاذية والانتقائية. وهي أيضا لديها القدرة على تحمل درجات حرارة عالية وظروف كيميائية قاسية. وتم إعداد هذه الأغشية (CMS) من خلال عملية تعرف باسم الانحلال الحراري.

الهدف الاساسي من هذا العمل البحثي هو إعداد أغشية الكربون المناخل الجزيئي (CMS) بكفاءة لفصل الأكسجين وتحسين أداء عملية الفصل باجراء عدد من العلاجات المختلفة. تم تصنيع هذه الأغشية من خلال الانحلال الحراري لغشاء البوليميد (KAPTON) التجاري. وكذلك تم ضبط متغيرات هذا الانحلال الحراري كسرعة التسخين، مدة التحلل، درجة الحرارة، والجو من أجل الحصول على المواصفات الأفضل للأغشية المصنعة.

في هذه الدراسة تم تطبيق نوعين من المعالجات المسبقة (الحرارية و الكيميائية) للأغشية البوليمارية، KAPTON، قبل خطوة الانحلال الحراري. أولاً، تم معالجة هذه الاغشية مسبقاً بالمادة الكيميائية: N-Methyl Pyrrolidone (NMP). وقد ادت هذه المعالجة الى تحسين إنتقائية أغشية الكربون المناخل الجزيئي (تصل الى 10.81) مع الاحتفاظ بنفاذية عالية (26 barrers). ثانياً، قد تم تعريض الغشاء KAPTON إلى المعالجة الحرارية في بيئة الأكسدة (الهواء) على الدرجة المثوية 350°C لمدة ساعة واحدة. هذه الأكسدة، بالتسخين الحراري، أدنت الى زيادة نفاذية غشاء ال CMS لتصل الى 50 barrers. لتحليل هذه الاغشية تم إستخدام المجهر الالكتروني الماسح (

(SEM), التحليل الحراري الوزني (TGA), محول مطياف فورييه للأشعة تحت الحمراء (FTIR) و جهاز انحراف الأشعة السينية (XRD). ولأول مرة من خلال هذه الاختبارات ان هذه الأغشية تحمل خصائص الغرلة الجزيئية في فصل الأوكسجين والنترجين.

# CHAPTER 1

## INTRODUCTION

### 1.1 GAS SEPARATION

Since the past 40 years gas separation become a major industrial application of membrane technology. The market of membrane based gas separation in the year 2010 was expected to be 350 million USD but the actual market value exceeded than what is expected and reached a total of 500 million USD [1, 2]. This shows the growing demand for gas separation. Currently, almost every known gas is being isolated for different applications. Various gas pairs separated employing membranes and their uses are shown in the Figure 1 [3].

Gas pair	Area of application
O <sub>2</sub> /N <sub>2</sub>	Oxygen enrichment, inert gas generation
H <sub>2</sub> /hydrocarbon	Refinery hydrogen recovery
H <sub>2</sub> /N <sub>2</sub>	Ammonia purge gas
H <sub>2</sub> /CO	Syngas ratio adjustment
CO <sub>2</sub> /hydrocarbon	Acid gas treatment, greenhouse gas capture
H <sub>2</sub> O/hydrocarbon	Natural gas dehydration
H <sub>2</sub> S/hydrocarbon	Sour gas treating
He/hydrocarbon	Helium separation
He/N <sub>2</sub>	Helium recovery
Hydrocarbon/air	Hydrocarbon recovery
H <sub>2</sub> O/air	Air dehumidification

Figure 1 Gas Pairs Separated Using Membranes and Their Applications [3]

Gas separation process such as  $H_2/N_2$  separation in the ammonium-production process has been commercialized since 1980. Recently, the separation of hydrogen from carbon dioxide has also become of considerable interest as it is a clean source of energy. At present, flue gas (mainly  $CO_2$  and  $N_2$ ), which is generated from power plants, accounts for the majority of man-made  $CO_2$  emissions [4]. Because of concern of global warming, there is also considerable interest in developing improved methods for separating and capturing  $CO_2$  from flue gas. Figure 2 shows important milestones achieved in the gas separation technology since 1850, when the graham's law of diffusion is discovered.

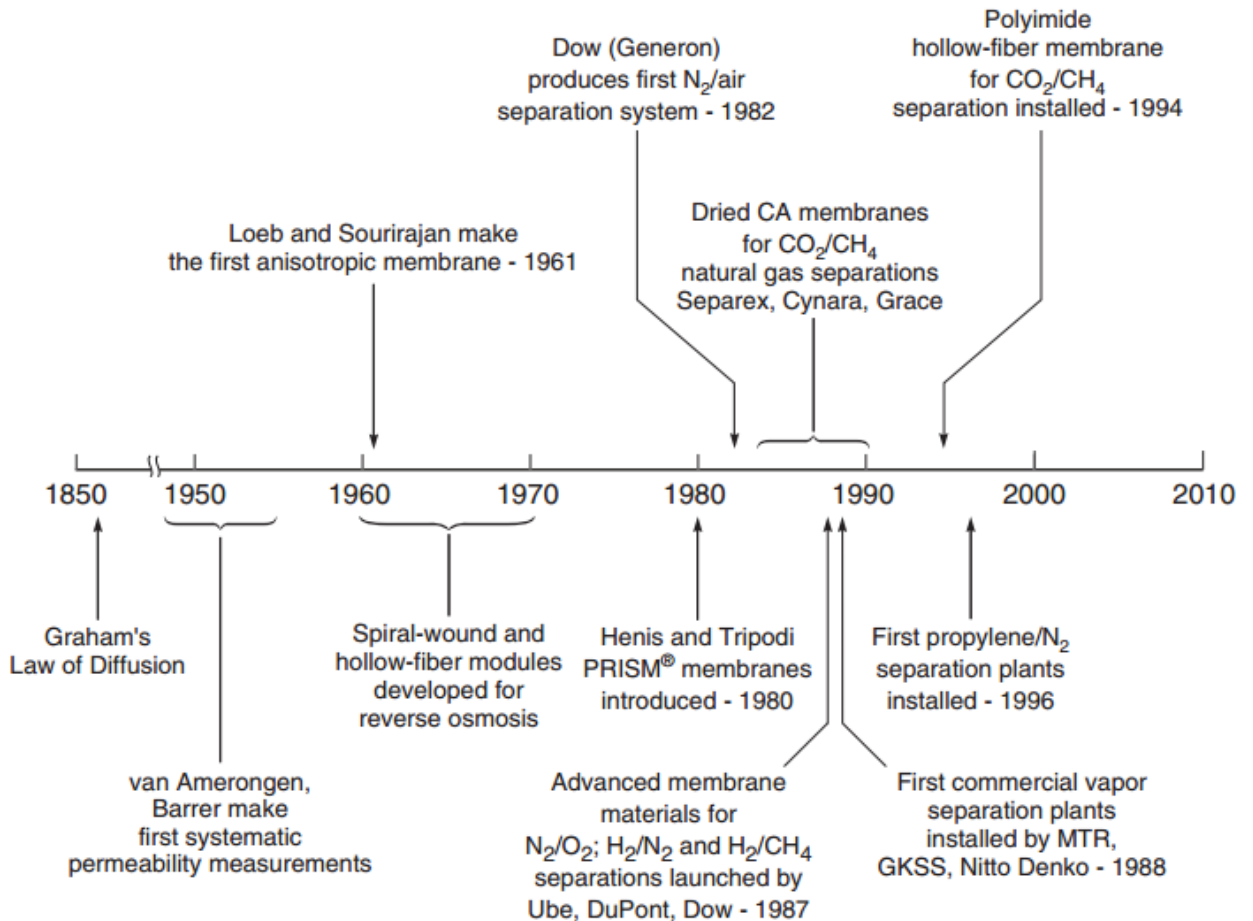


Figure 2 Important Milestones Achieved in Gas Separation

## **1.2 CONVENTIONAL GAS SEPARATION TECHNOLOGIES**

Cryogenic distillation and sorption methods were the two main technologies used before the emergence of membrane technology.

### **1.2.1 SORPTION PROCESSES**

Amine scrubbing is one of the sorption method used to separate the gases. In which an absorbent (Scrubber) is used to absorb a gas, the absorbed gas is then collected by regenerating the scrubber at elevated temperatures [5]. Even though this process is simple it requires large energy to regenerate the scrubber and also it involves large capital cost. In addition to amine scrubbing there are other sorption processes such as pressure swing absorption (PSA), Temperature swing adsorption (TSA) and vacuum swing adsorption (VSA). In these processes the gases are captured by solid adsorbents, In a recent review Razaei et al [6] summarized various structured adsorbents and their applications in adsorptive processes. and their applications in gas separation. The captured gas is then released by reducing the pressure (in PSA) or increasing the temperature (in TSA) or releasing the vacuum (in VSA) [7-9]. In these processes highly porous materials are used. Zeolites, zeolitic imidazolate frame works (ZIFs), metal organic frame works (MOFs), carbon molecular sieves, activated carbon, and alumina are some of the absorbents used in these processes. High energy consumption and deteriorating efficiency of the absorbents are the main limitations of these methods.

## **1.2.2 CRYOGENIC DISTILLATION**

Cryogenic distillation found its first application for gas separation in the early 20<sup>th</sup> century, when for the first time Carl Linde employed Cryogenic distillation to separate O<sub>2</sub>/N<sub>2</sub>. In cryogenic distillation the gases are separated by the difference in their boiling points. This method is mostly used because of its ability to produce high purity gases [10]. However, the cryogenic distillation modules require a large capital cost as they consists expansion turbines and compressors [11]. Moreover, a lot of energy is consumed to cool the gases to below their boiling points which limits their use in large scale gas separation plants [12]. Apart from these two conventional technologies membrane based separation evolved as an efficient alternative for gas separation.

## **1.3 MEMBRANES FOR GAS SEPARATION**

### **1.3.1 ADVANTAGES OF CHOOSING MEMBRANES OVER OTHER GAS SEPARATION TECHNOLOGIIES**

Comparing to the traditional technologies, membrane based separation process has the following benefits.

- ✓ Membrane based separation is environmentally clean and energy efficient technology.
- ✓ Simple equipment design and hence, involves low capital investment.
- ✓ Process is completely enclosed, thereby minimizing direct and fugitive emissions.
- ✓ System is compact, modular and easily transportable.

- ✓ Low operating cost, and easy to scale up for industrial use.
- ✓ Reduces the energy demand because only the fraction of the liquid needs to be vaporized.
- ✓ Opportunity for recovering concentrated organics.
- ✓ Preparing asymmetric structure with ease.

### **1.3.2 MEMBRANES**

Over the past few decades membranes were used in various separation processes such as ultrafiltration, dialysis, desalination, reverse osmosis, dehumidification and gas separation. The word membrane is derived from the Latin word, *membrana* which means a skin[13]. Nowadays this word is employed to describe thin flexible sheet or films, acting as a selective barrier between two phases [14].

The main function of the membrane is to control the permeation rate of a chemical substance through it [15]. In other words, it is a discrete thin barrier that controls the permeation of chemical species while in contact with it. This barrier (Membrane) can be homogenous (e.g single layered) or they can be heterogeneous (e.g combination of two or more layers). The gas feed is given to the upstream side and is maintained at higher pressure whereas the downstream is maintained at lower pressures or vacuum. This pressure difference develops a concentration gradient across the membrane which acts as a driving force to facilitate the diffusion of the gas species through the membrane. The gas species diffused through the membrane is called permeate. A schematic of membrane separation process can be seen in Figure 3.

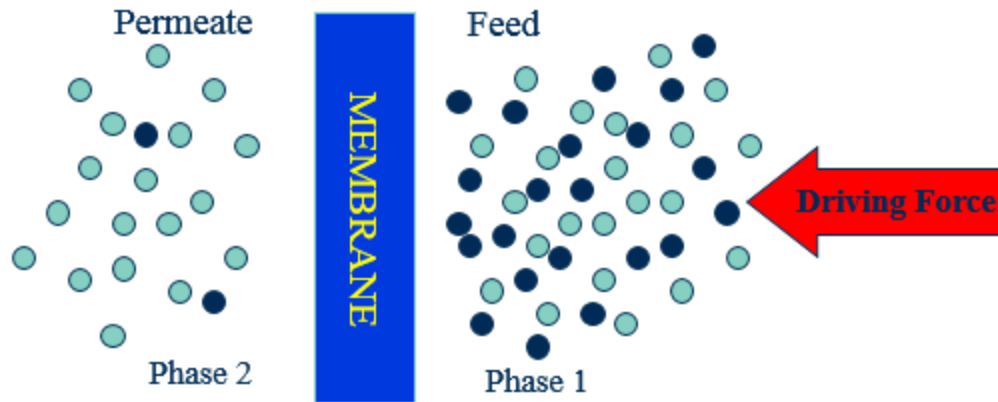


**Figure 3 Schematic of Membrane Separation.**

There are many advantages of choosing membranes when compared to other (non-membrane) separation processes such as small equipment size, ease of operation, eco-friendly, reliability and more over less energy consumption. As a first classification, membranes can be divided into two groups: synthetic and biological membranes. Synthetic membranes further divided into organic membranes (made of polymers) and inorganic membranes (made of metals, alumina etc.).

### **1.3.2.1 Polymeric Membranes**

Polymeric membranes are most commonly used for gas separation because of their reproducibility, mechanical strength, economical processing capacity and flexibility [16]. Depending upon the structure, polymeric membranes can be classified into porous and nonporous membranes [17]. Porous membranes have interconnected pores distribution due to which these membranes are highly permeable but are less selective. On the contrary, dense nonporous membranes are less permeable but are highly selective.

Polymeric membranes can also be classified into rubbery and glassy based on the polymer material used in the membrane preparation.

In the early years of membrane studies only natural polymers like natural rubber, gutta percha and gelatin was used. Poly(dimethyl siloxane) (PDMS), ethylene propylene rubber (EPDM), silicon rubber, poly phosphazene (PPZ) are few of the rubbery polymers used for oxygen separation. Since the advent of polymer science in the middle of 20<sup>th</sup> century researchers used synthetic polymers for various applications including gas separation. During 1960s to 1980s different semi crystalline polymers known as polyolefins were used for gas separation applications. Low density poly ethylene (LDPE), High density poly ethylene (HDPE), poly (4-methyl pentene) and polypropylene are few examples of semi crystalline polymers. Glassy polymers such as Cellulose acetate (CA), Polysulfone (PSf), Polyimide (PI), Polyethersulfone (PES) and polyamides (PA) were also used for gas separation applications [2, 18, 19]. However, the use of polymeric membranes is limited due to physical aging [20, 21] , plasticization behavior [22, 23] , poor chemical and thermal stabilities.

### **1.3.2.2 Inorganic Membranes**

Inorganic membranes possess unique perm-selective properties for gases with good chemical stability when compared to the polymeric membranes. Inorganic membranes are fabricated by metals, ceramics or pyrolyzed carbon. The first large scale gas separation membrane module using inorganic membrane was developed by Manhattan project in 1940s. Zeolites, Metal organic frameworks (MOFs), Carbon molecular sieves (CMSs), Zeolite imidazolate frameworks (ZIFs) and Silica are some of the inorganic

membranes. Carbon molecular sieves are good candidates for gas separation with high selectivity due to narrow pore distribution. The separation properties of these inorganic membranes lie far beyond the upper-bound limit for oxygen nitrogen separation [24-26]. However, brittleness, difficult preparation procedures (thermal programming for pyrolysis, zeolite crystallization, controlling the inert atmosphere etc), less reproducibility of properties and high cost of preparation are some of the limitations of inorganic membranes [27-30].

## **1.4 CARBON MOLECULAR SIEVES**

In general carbon membranes can be divided into 2 categories un-supported and supported carbon membranes with different configurations such as flat sheet, hollow fiber and capillary membranes. Most of the carbon membranes produced until 1990 were flat sheet membranes, the production of carbon hollow fiber membranes, carbon capillary membranes and carbon supported membranes supported on tubes started in the middle of 1990s [31]. In 1991 L.M Robeson reported that the performance of the membranes is limited by an upperbound trade-off and subsequently updated it in 2008 for different gas pairs like  $O_2/N_2$ ,  $H_2/N_2$ ,  $CO_2/CH_4$ ,  $H_2/CH_4$  and  $H_2/CO_2$  [32, 33]. Figure 4 shows Robesons plot for  $O_2/N_2$  separation containing available data points of various membranes, in which Permeability (P) and selectivity ( $\alpha$ ) are abscissa and ordinate respectively.

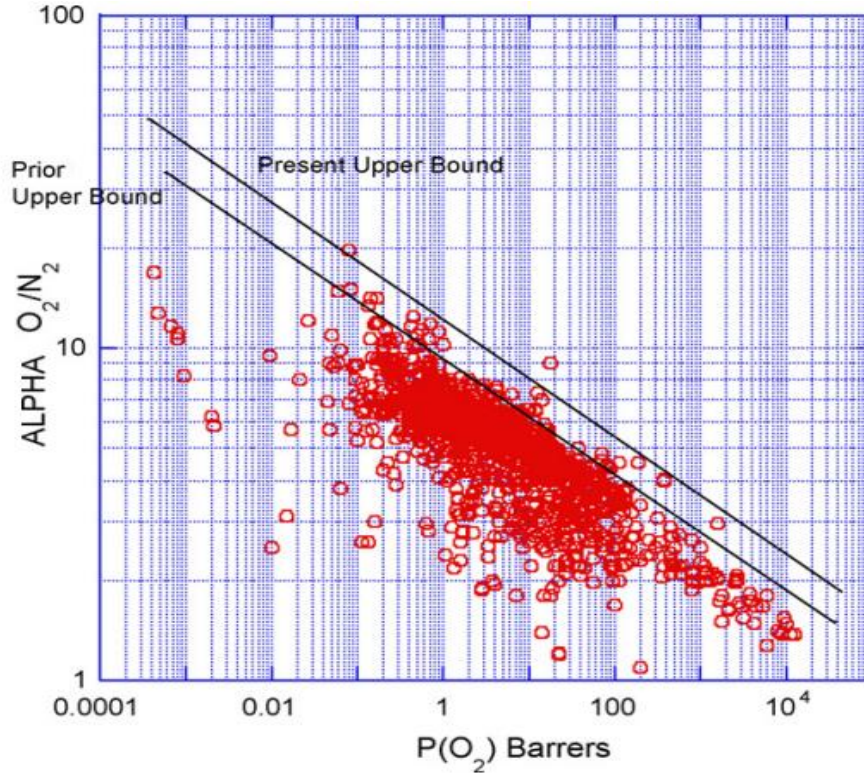


**Figure 4 Robeson Upper Bound**

In 1996 Koros and co-workers reported that CMS membranes had good separation performance for gas separation which surpass the Robeson's upper bound [34]. The research on carbon membranes intensified after Koresh and Soffer had successfully fabricated crack-free hollow fiber membranes by pyrolyzing cellulose hollow fibers.

Among the inorganic membranes reported so far CMS membranes are capable of withstanding high temperatures and harsh chemical conditions due to their inert inorganic carbon matrix. In addition, the separation properties of CMS membranes lie far beyond the Robeson's upper-bound limit for oxygen nitrogen separation [24-26]. CMS membranes are prepared by a process known as pyrolysis in which a suitable precursor is heated up to a certain temperature in an inert atmosphere. CMSM usually have narrow

pore size distribution with selective pores (constrictions) in the range of 0.3-0.5 nm, responsible for the molecular sieving properties of the membranes. These constrictions allow the passage of smaller permeants in detriment of bulkier permeants, which are retained. A slit shaped pore in the CMS membrane is illustrated in the Figure 5 [35]. Oxygen molecule can rotate about both of its axes and move easily through the pore whereas nitrogen molecule can only rotate about one of its axes. Which means nitrogen have less degrees of freedom if the pore size is close to the width of the nitrogen molecule which increases the oxygen/nitrogen selectivity. On the other hand most of the conventional polymers have same degrees of freedom for oxygen and nitrogen molecules, which are not so useful in oxygen/nitrogen separation [34].

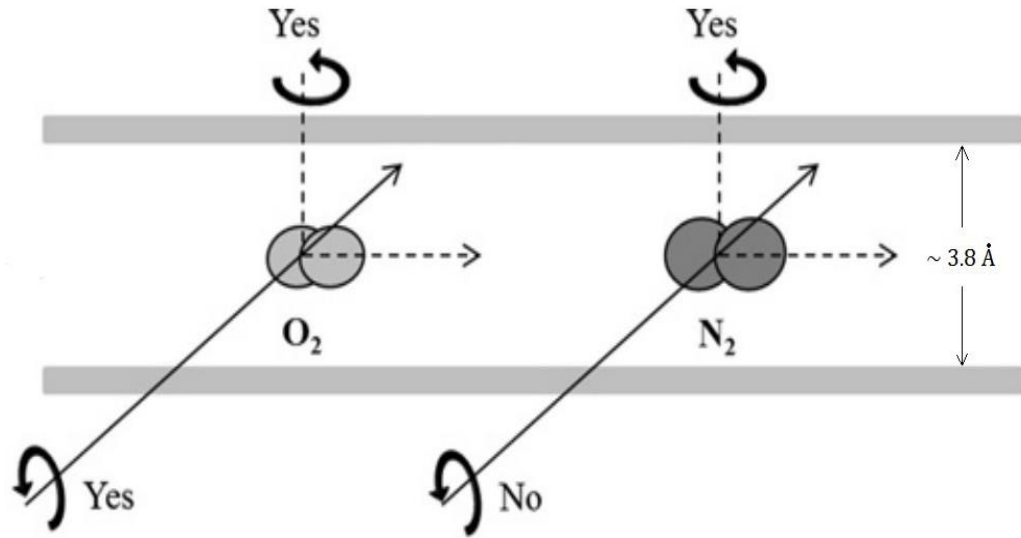


Figure 5 Illustration of Degrees of Freedom of  $O_2$ ,  $N_2$  Molecules in Slit-Shaped Pore in CMS Membrane.

According to a review by Saufi and Ismail [36] there are six different steps to obtain high performance CMS membranes as seen in Figure 6. The gas separation performance of carbon molecular sieves is affected by many factors such as pyrolysis temperature, polymer precursor, thermal soak time, heating rate, pretreatment and post treatments [37-40].

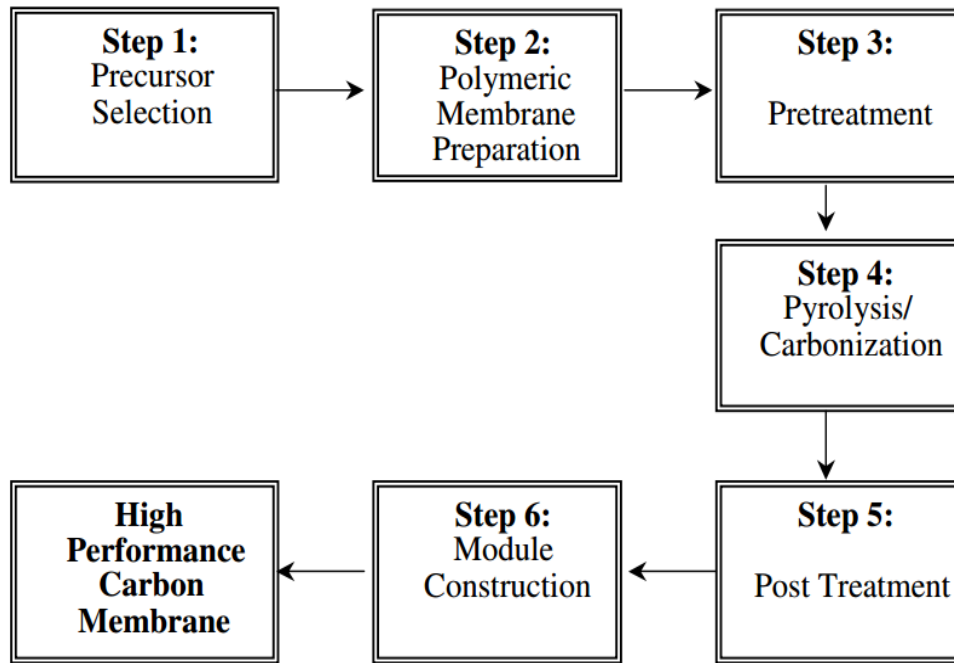
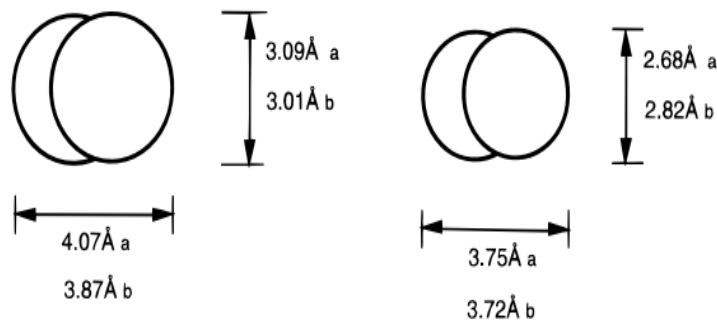


Figure 6 Steps Involved in the Successful Fabrication of CMS[36]

## 1.5 OXYGEN SEPARATION

Oxygen/nitrogen separation using polymer membranes is a rapidly growing field since the last few decades. This is also called as air separation, which is one of the largest gas separation process. Oxygen enriched air finds its application in refineries, in medical field, chemical industries and food packaging industries etc. Use of oxygen enriched air

(containing 25-30% oxygen) as a gasification agent in furnace improved the energy efficiency of the furnace [41, 42]. As the kinetic diameter of these gas molecules is very similar (nitrogen kinetic diameter is 3.64 Å whereas oxygen kinetic diameter 3.46 Å) so it is difficult to achieve size selectivity in membrane processes. Diatomic molecules like O<sub>2</sub> and N<sub>2</sub> have spherocylindrical structures. The lengths and widths of nitrogen and oxygen molecules is given in Figure 7, which is adopted from Singh et al [34].



**Figure 7 Molecular Sizes of N<sub>2</sub> and O<sub>2</sub>.**

In the air separation using cryogenic distillation, the cost of the process is determined by the amount of oxygen blend with the air to get required air enrichment. Which means that membranes used for air separation are taking the feed from the atmosphere containing only 21% oxygen can be counted as a credit. This fraction is called the equivalent pure oxygen (EPO<sub>2</sub>) basis. EPO<sub>2</sub> is defined as the amount of pure oxygen that must be mixed with normal air to obtain oxygen-oxygen enriched air (OEA). As an example, if a membrane produces 40 percent OEA, only the amount of oxygen added is counted, that is 24.1%.

Commonly pure oxygen is produced in two stages, researchers such as Baker [19] and Budd [43] are focused on developing new polymers which can exhibit good transport

properties such as high permeability and selectivity fluxes so as to develop production of O<sub>2</sub> in a single stage. A schematic of single and two-stage oxygen separation process can be seen in Figure 8.

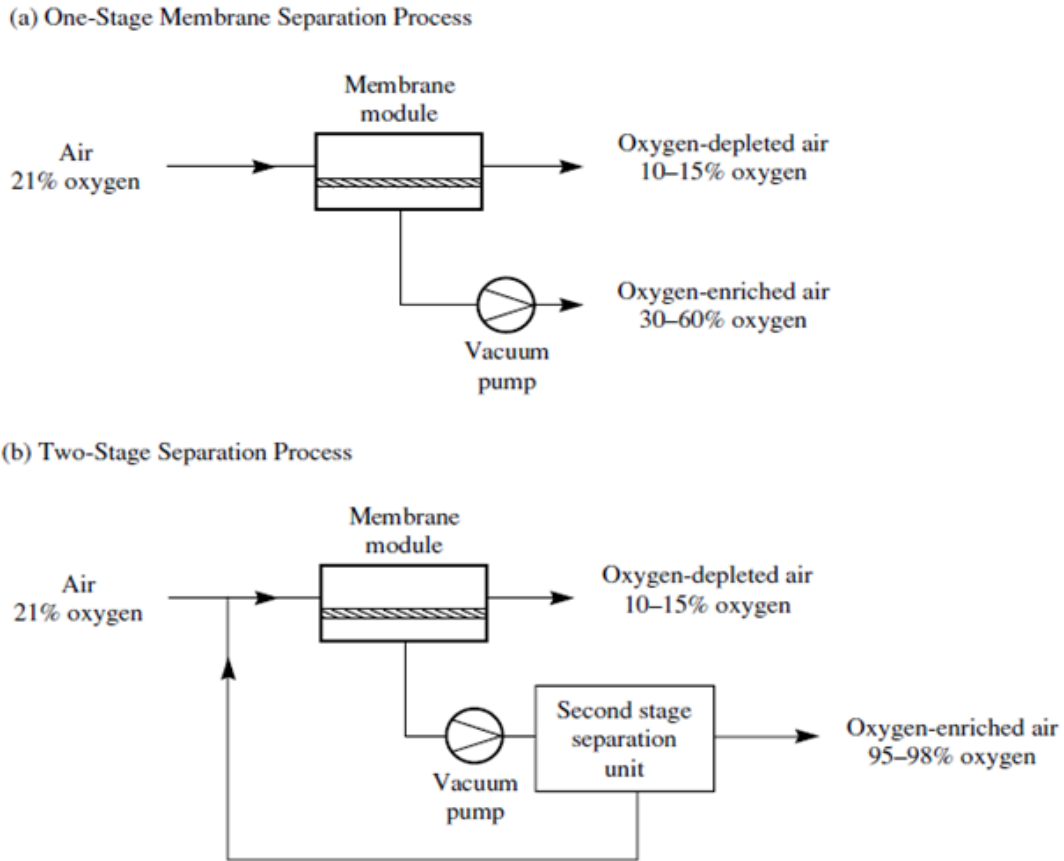


Figure 8 Single and Two-Stage Oxygen Separation Process.

During the last two decades dozens of new polymers have been described in the literature, which have been developed for gas separation. In spite of the production and evaluation of hundreds of new materials, more than 90% of current commercial membranes are made from fewer than 10 membrane materials [19]. The commercial membrane materials and their separation performances are tabulated in Table 1 [44]. All the commercial membranes separate gas mixtures by the solution diffusion mechanism. It

is clear from the Figure 4 and Figure 9 that very few polymers are located above the desired upper bound due to their low selectivity. Carbon molecular sieve (CMS) membrane materials are attractive alternatives because they offer very high selectivity and permeabilities.

**Table 1 Commercial Membranes for Oxygen Separation[44].**

Polymer	Permeability at 30°C (Barrer*)				
	H <sub>2</sub>	N <sub>2</sub>	O <sub>2</sub>	CH <sub>4</sub>	CO <sub>2</sub>
Cellulose acetate	2.63	0.21	0.59	0.21	6.3
Ethyl cellulose	87	8.4	26.5	19	26.5
Polycarbonate, brominated		0.18	1.36	0.13	4.23
Polydimethylsiloxane	550	250	500	800	2700
Polymide (Matrimid)	28.1	0.32	2.13	0.25	10.7
Polymethylpentene	125	6.7	27	14.9	84.6
Polyphenyleneoxide	113	3.81	16.8	11	75.8
Polysulfone	14	0.25	1.4	0.25	5.6

The data in table 1 plotted on Robeson upper bound as can be seen in figure 8.

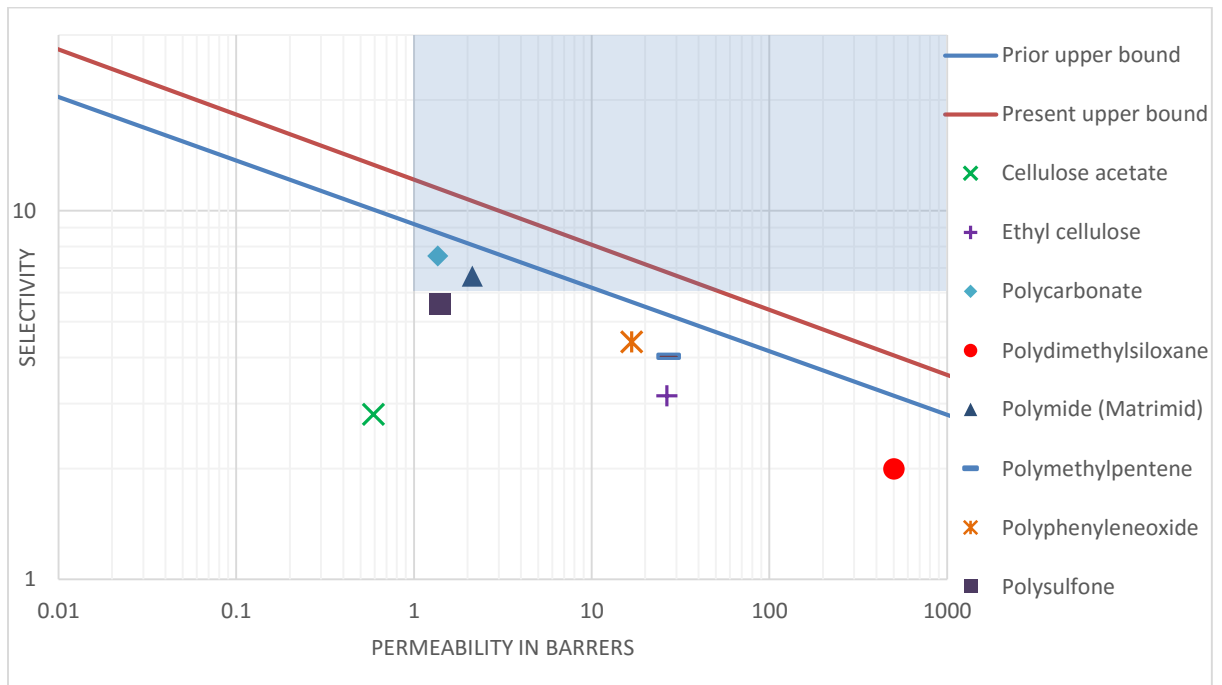


**Figure 9 Oxygen Separation Performance of Commercial Membranes.**

## 1.6 OBJECTIVES

Carbon molecular sieves (CMSs) are highly porous materials and possess ultra micropores having dimensions that are of the same order of magnitude as the molecular sizes of gas molecules. These pores can impart entropic selectivity to the CMSM by restricting the degrees of freedom of gas molecules. The distinctive feature of CMSM is that, by employing different pyrolysis conditions, they can be tailored in order to yield different gas permeation properties. The pore network can also be adjusted or tuned by combining several pre-treatment or post-treatments leading to the desired pore size distribution. Carbon molecular sieves with good selectivity can surpass the upper bound as mentioned earlier. The objective of this study is to obtain efficient self-supporting CMS membranes, whose separation performance can surpass the Robeson's upper bound for oxygen separation, which can be achieved by the following ways.

- (1) Optimizing the pyrolysis parameters to obtain a CMS with satisfactory gas separation performance.
- (2) Studying the effect of chemically treating the polymer on the permeation properties of CMSM.
- (3) Optimizing pre heat treatment of the polymer precursor prior to the pyrolysis process in order to achieve desired properties of the membrane.
- (4) Studying the effect of post heating the membrane after the pyrolysis process.

## **CHAPTER 2**

### **LITERATURE REVIEW**

#### **2.1 GAS TRANSPORT IN MEMBRANES**

Dense as well as porous membranes can be employed for gas separation. In dense membranes the gas permeation is governed by solution diffusion model. In general, gas transport phenomenon in polymer membranes contains following steps [45]

1. Diffusion of the gases across the boundary layer of the membrane.
2. Sorption of the gases.
3. Diffusion of the gases inside the polymer membrane.
4. Desorption of gases on the permeate side.
5. Diffusion out of the boundary layer of the downstream side.

The transport phenomenon through the membranes varies with different pore sizes[46]. In Figure 10 three types of porous membranes having different pore sizes are shown. If the pore size is large (i.e from 0.1 to 10  $\mu\text{m}$ ) the gas permeation occurs by convective flow, where no separation takes place. If the pore size is less than 0.1  $\mu\text{m}$ , diffusion happens by Knudsen diffusion mechanism. Finally, if the membrane pores are extremely small (in the range 5–20  $\text{A}^\circ$ ) then gases separation is done by molecular sieving [47].

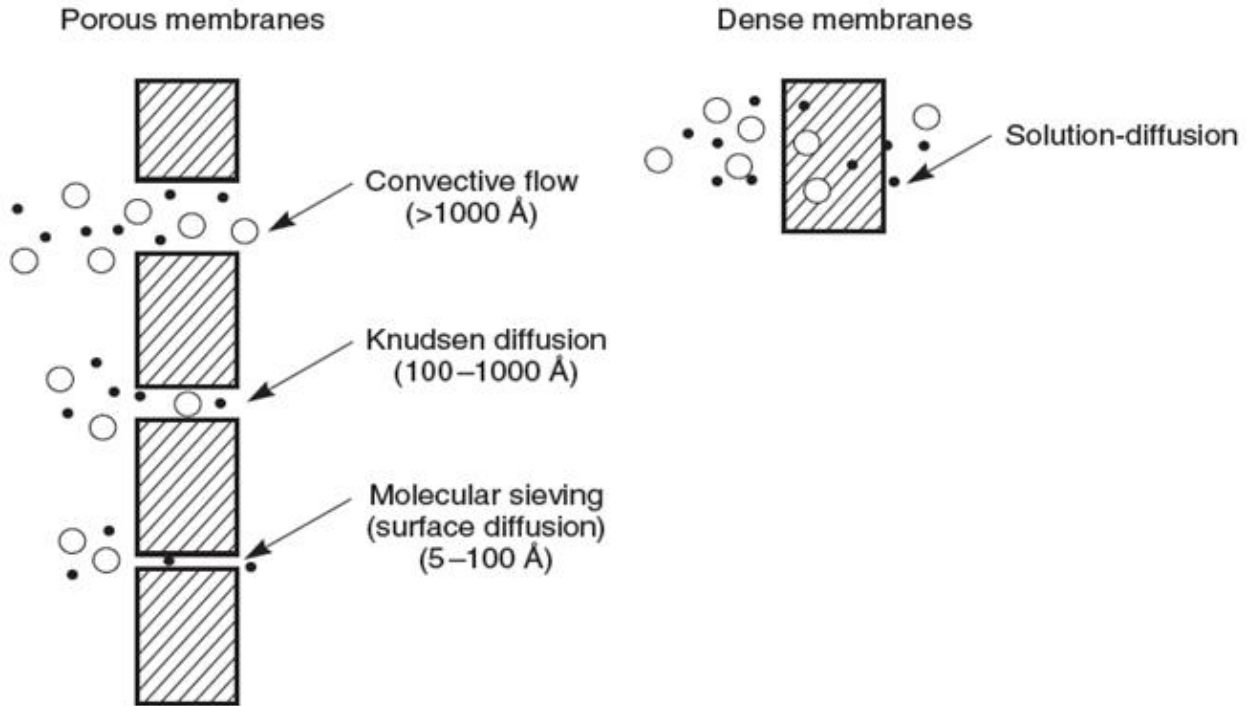


Figure 10 Gas Permeation Mechanisms.

## 2.2 GAS TRANSPORT MECHANISMS

### 2.2.1 CONVECTIVE FLOW

As shown in Figure 10, convective flow dominates when the pore diameter is larger than 1000 Å, and this can be described by Poiseuille's law according to equation:

$$j = \frac{r^2 \varepsilon}{8\eta} \times \frac{[p_0 - p_l][p_0 + p_l]}{l \cdot RT} \quad (2.1)$$

Here  $J$  is the gas flux,  $r$  is the pore radius,  $\eta$  is the viscosity of the gas,  $l$  is the pore length,  $\varepsilon$  is the porosity of the membrane and  $p_0$  represent the absolute pressure of gas species at the beginning of the pore ( $x=0$ ),  $p_l$  represent the absolute pressure of gas species at the end of the pore ( $x=l$ ).  $T$  is temperature and  $R$  is the ideal gas constant. For a membrane everything is constant except  $\eta$ , therefore the gas selectivity for any two gases  $i, j$  can be expressed by equation:

$$\alpha_{ij} = \frac{\eta_i}{\eta_j} \quad (2.2)$$

As the viscosity  $\eta$  of different gaseous species is very small, Convective flow gives little gas selectivity.

### 2.2.2 KNUDSEN DIFFUSION

If the diameter of the pores is in the range of 100 to 1000 Å, the transport is governed by Knudsen diffusion. In a Knudsen flow, the gas molecules have more collisions with pore walls than with other gas molecules [48]. The flux of the gas is then given by equation:

$$j = \frac{4r\varepsilon}{3} \left( \frac{2RT}{\pi M} \right)^{1/2} \cdot \frac{p_0 - p_l}{l \cdot RT} \quad (2.3)$$

where,  $r$  is the pore radius,  $M$  is the molecular weight of the gas molecule,  $l$  is the pore length,  $\varepsilon$  is the porosity of the membrane and  $p_0$  represent the absolute pressure of gas species at the beginning of the pore ( $x=0$ ),  $p_l$  represent the absolute pressure of gas species at the end of the pore ( $x=l$ ).  $T$  is temperature and  $R$  is the ideal gas constant. It

can be noticed that the permeability of a gas via Knudsen diffusion is proportional to  $(M)^{-1/2}$  therefore, the gas selectivity for any two gases can be expressed by the inverse square root of the ratio of their molecular weight.

### 2.2.3 MOLECULAR SIEVING EFFECT

When the diameter of the pore is very small (5 to 100 Å) then the gas transport happens by the molecular sieving effect. The membranes governed by this mechanism allow only smaller gas molecules by blocking the bigger ones[49]. The sorption effect is normally ignored when molecular sieving effect is dominating. The flux and diffusion coefficient that are associated with molecular sieve membranes can be expressed as follows:

$$J = \frac{\Delta p}{l \cdot RT} \cdot D_o \cdot \exp\left(\frac{-E_a}{RT}\right) \quad (2.4)$$

$$D_o = g_d d_p \lambda^2 \frac{kT}{h} \exp\left(\frac{S_{a,d}}{R}\right) \quad (2.5)$$

Here J is flux,  $E_a$  is the activation energy,  $D_o$  is the diffusion coefficient of the membrane, for permeation,  $g_d$  is probability that a molecule can make a jump in the right direction given that jump length is  $d_p$  is jump length,  $S_{a,d}$  is the activation,  $h$  and  $k$  are Planck's and Boltzmann's constants respectively. Based on these equations, it can be noticed that increasing temperatures will increase the flux and decrease the selectivity of the gases.

## 2.2.4 THE SOLUTION-DIFFUSION MODEL

Thomas Graham gave the first description of the solution-diffusion model, and his work on membranes led to Graham's law of diffusion. In the 1940s to 1950s, Barrer, van Amerongen, Stern, Meares and others laid the foundation of the modern theories of gas permeation[50, 51]. This model applies to dense polymeric membranes. Polymer membranes consists of dynamic transient gaps, which result from the thermal motions of polymer chains. These gaps allow gas molecules to diffuse through polymeric membranes.

If a concentration gradient is established across some arbitrary reference section in the polymer, a net transport of penetrant occurs in the direction of decreasing concentration as illustrated in Figure 11. This phenomenon can be described in terms of Fick's first law of diffusion according to which the diffusive flux,  $J$  (the amount of penetrant passing through a plane of unit area normal to the direction of flow during unit time) in the  $x$ -direction of flow is proportional to the concentration gradient where  $D$  is the diffusion coefficient and ' $c$ ' the concentration of the diffusing molecule. This equation is applicable when the diffusion is in the steady state.

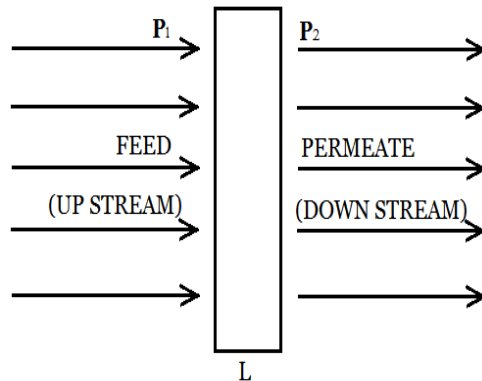


Figure 11 Illustration of Membrane

From Fick's first law,

$$J = -D \frac{dc}{dx} \quad (2.6)$$

Where,  $D$  is the diffusion coefficient and  $\frac{dc}{dx}$  is concentration gradient

$$\Rightarrow J \cdot dx = -D \cdot dc$$

Integrating on both the sides

$$\Rightarrow J \cdot \int_0^l dx = -D \cdot \int_{c_1}^{c_2} dc$$

As the thickness of membrane  $dx$  changes from '0' to 'l' concentration changes from  $dc$  changes from 'c1' to 'c2'

$$\Rightarrow J \cdot (l - 0) = -D \cdot (c_2 - c_1)$$

$$\Rightarrow J = \frac{D \cdot (c_1 - c_2)}{l} \quad (2.7)$$

From Henry's law we have,

$$C = S \cdot p \quad (2.8)$$

Where,  $p$  is the partial pressure and  $S$  is the solubility coefficient,

Substituting equation (2.8) in (2.7), we get

$$\Rightarrow J = \frac{D(S \cdot p_1 - S \cdot p_2)}{l}$$

$$\Rightarrow J = \frac{D \cdot S (p_1 - p_2)}{l}$$

Where  $p_1$  and  $p_2$  are upstream and downstream partial pressures

$$\Rightarrow J = \frac{P (p_1 - p_2)}{l}$$

Where  $Permeability (P) = D \cdot S$

$$\Rightarrow P = \frac{J \cdot l}{(p_1 - p_2)} \quad (2.9)$$

And we know that,

$$J = \frac{n}{A \cdot t} \quad (2.10)$$

Where,  $n$  is the amount of gas permeating,  $A$  is the area of cross section and  $t$  is the time in seconds

Substituting equation (2.10) in (2.9), we get

$$P = \frac{n \cdot l}{A \cdot t \cdot (p_1 - p_2)} \quad (2.11)$$

From ideal gas law, we have  $p \cdot V = n \cdot R \cdot T$

$$n = \frac{p \cdot V}{R \cdot T} \quad (2.12)$$

Substitute (2.12) in (2.11), we get  $P = \frac{p \cdot V \cdot l}{R \cdot T \cdot A \cdot t \cdot (p_1 - p_2)}$

As the pressure is varying with time we can write the above equation as,

$$P = \frac{V}{R \cdot T} \cdot \frac{1}{A} \cdot \frac{l}{(p_1 - p_2)} \cdot \left( \frac{dp}{dt} \right) \quad (2.13)$$

Converting the units to barrers,

$$\therefore P = 22414 \cdot 10^{10} \frac{V}{R \cdot T} \cdot \frac{1}{A} \cdot \frac{l}{(p_1 - p_2)} \cdot \left( \frac{dp}{dt} \right) \quad (2.14)$$

Where, P is the Permeability ( barrers ) , V is the Volume of the downstream chamber (in  $\text{cm}^3$  ) , T is the Temperature (in K ) , R is gas constant ( $R = 6236.56 \frac{\text{cm}^3 \cdot \text{cmHg}}{\text{mol} \cdot \text{k}}$  ) , A is Effective area of the membrane (in  $\text{cm}^2$  ) , l is the Membrane thickness (in cm ) ,  $p_1$  is Feed pressure (in mbar ) ,  $p_2$  is Permeate pressure (in mbar ) and  $\frac{dp}{dt}$  is the slope of the Permeability vs time graph ( $\frac{\text{mbar}}{\text{sec}}$ ).

### 2.3 SELECTION OF PRECURSOR

The selection of a suitable precursor for pyrolysis is an important task in the successful fabrication of a carbon molecular sieve. Same carbonization conditions on different precursors yield CMS with different properties. Researchers used various materials for the preparation of carbon membranes such as coal, resin, plants, pitch, graphite and polymers. The polymers used for the pyrolysis should meet certain requirements.

Firstly, it should be a thermosetting polymer and should be able to produce high carbon yield after carbonization. Secondly, it should decompose to form defect free (i.e without cracks or pin holes) carbon structure without softening or melting during the pyrolysis [52]. Different polymers used in the literature are poly acrylonitrile (PAN), polyimides, poly aramides, Cellulose acetates, poly furfuryl alcohol etc. Among these materials

polyimides are most commonly used precursors for the fabrication of CMS membranes because of their exceptional properties [53, 54]. Polyimides are high carbon containing polymers capable of withstanding high temperatures up to 350 °C without changing their shape. They have high glass transition temperature and decomposes before reaching to their melting point [55].

## **2.4 PRETREATMENT**

Pretreatment can be done in two ways i.e chemical and physical pretreatments. In chemical pretreatment process the polymer precursor is immersed in an appropriate chemical for a certain period. Hydrazine, ammonium chloride, hydrochloric acid and dimethyl formamide (DMF) are some of the most commonly used chemicals for pretreatment [52]. After the chemical treatment the polymer precursor is washed and dried. As an example, Tin et al.[26, 56] immersed polyimide Matrimid 5218 in cross linking reagent (solution of p-xylenediamine in methanol) for various time periods and observed that the pretreatment improved the selectivity of the CMS membrane. This cross-linking modification enhanced the mobility of the polymer chains and their structural arrangement to form micropores.

Stretching is one of the physical pretreatments methods applied to the polymer precursors before the carbonization. Oxidation treatment is one of the most popular and important pretreatment method in which a polymer precursor is heat treated under an oxidative agent such as oxygen or air, with the objective of avoiding an undesirable release of volatiles during pyrolysis, ensuring a final carbon membrane with maximized carbon

content and minimized pinholes. Which allows the polymeric precursor to retain its form and structure during pyrolysis as a result of the formation of crosslinks in the polymer that increase its thermal stability. Centeno and Fuertes [57] heat treated a phenolic resin in air (i.e oxidative environment) in a temperature range from 150 °C -300 °C for 2 hours. The permeation rate of the resultant CMS membrane is found to be improved significantly, this confirms the enlargement of pores on the CMS membrane. Sometimes the precursor is subjected to more than one pretreatment method to achieve the desired properties in a carbon membrane.

## **2.5 PYROLYSIS**

Sometimes pyrolysis is referred as carbonization, in this process a suitable precursor is heated up to a temperature (i.e carbonization temperature) at required heating rate in a controlled atmosphere. Volatile byproducts like H<sub>2</sub>, N<sub>2</sub>, CO<sub>2</sub>, NH<sub>3</sub> and H<sub>2</sub>O etc will be produced during pyrolysis. These byproducts cause a huge weight loss[58]. Generally, a polymer is pyrolyzed in an inert purge usually Ar, He or N<sub>2</sub>. The temperature is then increased up to 800 °C to 1000 °C.

The carbonization temperature should be changed according to the target gases to be separated [59]. Sometimes thermal soaking is carried out by holding the material for certain duration at a particular temperature. The gases evolved during the pyrolysis forms pores in the polymer. In order to obtain fine pore structure and increase the performance of the membrane several parameters can be controlled like thermal soaking time, pyrolysis environment, heating rate and pyrolysis temperature etc. After the pyrolysis the CMS membranes must be preserved in airtight bags so as to prevent them from physical

aging [60, 61]. If the membranes were left in ambient atmosphere for longer durations a regeneration step is required to reset the properties of the membrane [62, 63]. Various polyimides, their pyrolysis conditions and permeation properties are listed in the Table 2.

**Table 2 Various Polymers, Their Pyrolysis Conditions and Permeation Properties.**

Polymer precursors used for pyrolysis	Heating rate, Pyrolysis temperature, Holding time, Pyrolysis environment	Permeability	Selectivity	Reference
Matrimid ®	0.5°C/min, 450-700°C, 1h, Vacuum	5	6	[64]
Kapton	3°C/min, 800°C, -, -	1.2	4.62	[65]
Kapton	10°C/min, 1000°C, 2h, Vacuum	0.96	23.4	[59]
Poly(furfuryl)alcohol	-, 600°C, -, inert atmosphere	1.2-7.2	2.7-3.7	[66]
PFA	5°C/min, 450°C, 2h, Helium	1.45-2.74	2.2-6.4	[67]
Polypyrrolone	5°C/min, 800°C, 1h, Nitrogen	0.183	7.8	[68]
Polyimide (AP)	3.85°C/min, 800°C, 2h, -	23	12.3	[69]
Polyimide matrimid 5218	5°C/min, 500°C, 0.5h, Nitrogen	6.67	5.65	[70]
Polyimide Matrimid 5218	10°C/min, 800°C, 2h, Vacuum	227	7.6	[71]
Matrimid ®	4°C/min, 800°C, 2h, Vacuum	24	12.9	[72]
Polyimide BTDA-ODA-mPDA	3°C/min, 700°C, 1h, Argon	256	11	[25]
P 84 (commercial polyimide)	-, 800°C, 2h, Vacuum	158	8.9	[56]
BTDA-ODA	3°C/min, 800°C, 0.5h, Argon	61	15	[73]

## **2.6 EFFECT OF PYROLYSIS VARIABLES**

### **2.6.1 Effect of Pyrolysis Temperature**

The maximum temperature up to which the precursor is heated during the pyrolysis is known as the pyrolysis temperature which is also known as carbonization temperature. Generally the carbonization temperature is in between the decomposition temperature and the graphitization temperature of the precursor [74]. The variation of pyrolysis temperature affects several parameters which determine the perm selectivity of the membrane such as kinetics of the polymer, degradation of the byproducts and compactness of the turbostatic structure[58]. Islam et al [75] pyrolyzed sulfonated polyimides at Lower pyrolysis temperature (at 450 °C) and found that the resultant membranes possess flexible properties as polymeric membranes and good selectivity as in CMS membranes . Higher pyrolysis temperature tends to increase in selectivity due to narrower pore size distribution. DSC analysis on different membranes shown that at higher temperatures (up to 800 °C), approximately 95% of the carbon content was left [76]. Increase in pyrolysis temperature also tends to higher crystallinity, higher density and higher compactness. However, the interplanar spacing between the layers of carbon is reduced [77, 78].

### **2.6.2 Effect of Vacuum Atmosphere**

Generally, a vacuum or an inert purge gas is required to remove volatile gases and to prevent damage of the membranes during carbonization. Increasing the degree of vacuum by keeping the temperature constant, results in a membrane with high selectivity and

relatively low permeability[58, 76]. However, the change in selectivity depends up on the type of precursor. On the other hand, high permeability can be achieved using inert gas or lower degree of vacuum. Kiyono et al [79] pyrolyzed a polyimide 6FDA/BPDA-DAM in two different degrees of vacuums (0.005 torr and 0.042 torr) to obtain CMS membranes. The membranes pyrolyzed in lower degree of vacuum had high oxygen permeability (630 barrers) with low selectivity (8.8) whereas the membranes pyrolyzed in higher degree of vacuum had low permeability of oxygen (52 barrer) with comparatively high selectivity (10). Geiszler et al [80] used different pyrolysis atmospheres such as vacuum, argon, helium and carbon dioxide and found that the membranes pyrolyzed in vacuum atmosphere has more O<sub>2</sub>/N<sub>2</sub> selectivity.

### **2.6.3 Effect of Inert gas flowrate**

Use of inert purge in the carbonization process enhances the degradation of the precursor due to increased gas phase mass and heat transfer. Thus, pyrolysis in inert gas environment develops more porous structure in the CMS membrane, which enhances the permeability of the membrane. As the oxygen content in the inert purge increased, the weight loss is reported as to be decreased by W.J Koros et al[79]. At higher gas flow rates ( 200 cm<sup>3</sup>(STP) / min ) the gas permeability is high when compared to low purge flow rate in case of thin membranes ( 20 cm<sup>3</sup>(STP) / min ) [58]. On the contrary, flow rate has no impact on separation performance of dense CMS membranes[79].

#### **2.6.4 Effect of Soak Time**

The amount of time for which the precursor is held at the pyrolysis temperature is called thermal soak time. It can be adjusted to tune the separation characteristics of CMS membranes. Increase in soak time during pyrolysis leads to microstructural rearrangement, which affects the average porosity and the pore size distribution of the membrane. David et al [81] pyrolyzed PAN hollow fiber membranes and found that increase in the soaktime increased the permeability in early stage (up to 2 hours) then started decreasing after 2 hours. Increasing the thermal soak time decreased the permeability also reported by steel et al [72]. Higher soak time results in reduction in pore size due to sintering effect is reported elsewhere [82-84].

#### **2.6.5 Effect of Heating Rate**

The heating rate doesn't have any effect on the permeation properties of CMS membranes made at lower temperatures. However, at higher pyrolysis temperatures the carbon membranes pyrolyzed by different protocols shown improvement in gas transport properties[85]. Generally increasing the heating rate leads to reduction in pore size and thus increasing the selectivity[86]. Decreasing the heating rate slows down the by-product evolution rate and an increases the pyrolysis time thereby reducing the permeability. The permeability of the gases in the CMS membranes prepared from Kapton decreased with decrease in the heating rates from 13.3 °K/min to 1.33 °K/min as reported by Suda and Haraya [59]. Centeno et al [86] pyrolyzed phenolic resin at five different heating rates ranging from 0.5 °C/min to 10 °C/min and found that the selectivity increased with increase in the heating rate.

## 2.7 POST TREATMENT

The CMS membrane thus formed after the pyrolysis may not be selective if the size of the pore is larger than the gas molecules to be separated and it may not permeate the desired gas species through the membrane if the pores are smaller than the target gases to be separated. Therefore, there is a need to tune the pores and repair the defects of the CMS membranes by post treatment. Any defects in the membrane can be repaired by applying polymer coating on the CMS. To reduce the pore size or to close the pores Chemical vapor deposition can be employed. On the other hand, to enlarge the pores post oxidation heat treatment can be applied [87]. Steam activation also reported as a post oxidation procedure to finely tune the pores of the CMS membranes [88].

Oxidation of CMS membranes derived from BPDA-ODA polyimide at 300 °C in oxidative environment improved the gas permeation due to enlargement of the pores as reported by Hayashi [89] and Kusakabe [90] et al. In another research Hayashi et al [91] applied CVD through pyrolysis of propylene at 650 °C and this post treatment improved the O<sub>2</sub>/N<sub>2</sub> selectivity to 14.

# CHAPTER 3

## EXPERIMENTAL

### 3.1 POLYMER PRECURSOR

Polyimides are best suitable precursors for the fabrication of carbon molecular sieves as we have seen in the section 2.3. In general preparation of polyimides is very costly which limits their use in the preparation of CMS membranes. As an example, the monomer used in the synthesis of Kapton film (i.e 15wt% polyamic acid (PAA) solution in NMP) costs 385\$/1L at Sigma Aldrich. Therefore, instead of synthesizing the polymer in the laboratory selecting the polyimides which are commercially available in the market will be beneficial. Most of the polyimides are commercially available such as Ultem R 1000 (by general electric), Matrimid 5218 (by Ciba chemicals), Kapton (by DuPont) and P84 etc [92]. Kapton is available at 12\$/Square meter.

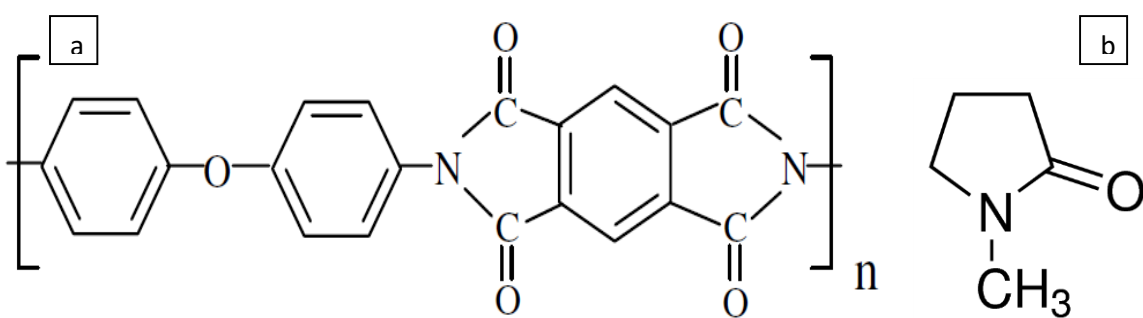


Figure 12 Chemical Structure of (a) Kapton (b) NMP

In our research a commercially available polyimide film Kapton (from Dupont) of thickness 1 mil (25  $\mu\text{m}$ ) is used as a precursor. The precursor has yellow color and a glass

transition temperature above 300 °C. The chemical structure of the Kapton film is given in (Figure 12) [59].

Prior to the pyrolysis the polymer is cleaned to remove any dust particles on it. Then it was cut in to circles of 32mm diameter in order to obtain the CMS membranes of diameter 25 mm after the pyrolysis. The final diameter of CMS is chosen so that, the membrane will fit easily in the permeation cell of one-inch diameter (i.e 25.4mm) and ease the permeability tests. The polymer is then sandwiched between the carbon plates to avoid wrinkle formation during the pyrolysis. The Kapton polyimide placed on the carbon support can be seen in the Figure 13.



**Figure 13 Polymer Precursors Prior to Pyrolysis**

### **3.2 PRE TREATMENT OF THE POLYMER**

The polymer films were subjected to two types of pre-treatments. The first pre-treatment is a heat treatment in an oxidative environment at different temperatures ranging from 250°C to 400°C. The other pre-treatment is a chemical treatment in various chemicals for 24 hours. The optimized pre-treatments and their description can be seen in Table 3.

**Table 3 Sample Names and Their Description**

s.no	Sample name	Type of treatment	Applied to	Duration	Description
1	KP	-	-	-	Raw Kapton film
2	CMS	-	-	-	Raw Kapton film pyrolyzed at 800 °C
3	CMS-HT-BP	oxidation heat treatment	Polyimide before pyrolysis	1 hour	The Kapton film heat treated at 350 C in a box furnace and then pyrolyzed at 800 °C
4	CMS-HT-AP	oxidation heat treatment	CMS after pyrolysis	1 hour	The Kapton film pyrolyzed at 800 °C then heat treated in a box furnace up to 350 °C
5	CMS-NMP-CP	Chemical treatment	Polyimide before pyrolysis	24 hours	The Kapton film kept in N-methyl pyrrolidone for 24 hours then cleaned with a tissue paper and pyrolyzed at 800 °C
6	CMS-NMP-IWT	Chemical treatment	Polyimide before pyrolysis	(12+12) hours	The Kapton film kept in N-methyl pyrrolidone for 12 hours then cleaned with water and dried, same thing repeated for a second time and then it was pyrolyzed at 800 °C

After the pre-oxidation heat treatment, the film expected to be free of any gases or solvents trapped in the film and also improve its thermal stability due to formation of crosslinks. Whereas, there are many reasons behind pre-treating the Kapton film with NMP prior to the pyrolysis.

Generally, polyimides are formed by crosslinking the monomers either chemically or thermally, in order to achieve the desired properties. Presence of small amount of NMP in the precursor improved the crosslinking reaction rate [93, 94]. In general, polyimides are prepared by casting a precursor solution on a support followed by thermal curing. Kapton is mostly prepared by casting a precursor solution of Polyamic acid (PAA) in NMP followed by stepwise thermal curing to induce cyclodehydration [95, 96]. It is established that the solvent NMP acts a plasticizer until it is removed by evaporation from the films. This is due to the formation of hydrogen bonding between NMP and Polyimide and also because of its high boiling point 202 C [97, 98]. It is also proven that presence of low molecular weight compounds such as NMP in the polymer films did not change the main structure of the polymer but promotes the segmental motion of the polymer chains (i.e it acts as a plasticizer) [99, 100].

The sample names are given according to the type of treatment done to the Kapton film (KP), in which HT refers to heat treatment and NMP is treatment with N-methyl pyrrolidone. Among the heat treated samples HT-BP refers to heat treatment before the pyrolysis and HT-AP denotes heat treatment after the pyrolysis. And also there are two different procedures in NMP treated samples in which NMP-CP stands for the polyimide cleaned with paper and NMP-IWT refers to the polyimide washed with water after the treatment.

### 3.3 CARBONIZATION

The pyrolysis setup is made as reported by Koros et al [79] to produce carbon molecular sieve membranes. The polyimide precursors were pyrolyzed in Carbolite CTF 12/100/900 furnace, which is a horizontal quartz tube furnace and can be heated up to a maximum temperature of 1200 °C. The carbon supports containing the membranes were carefully placed in the middle of the furnace tube for uniform distribution of heat throughout the samples. Then the tube is closed with the aluminum end caps from both the sides. One end cap is provided with the vacuum pump and a pressure gauge, whereas the other end cap is equipped with an external thermo couple and a vent. The setup can be visualized by the schematic as in Figure 14.

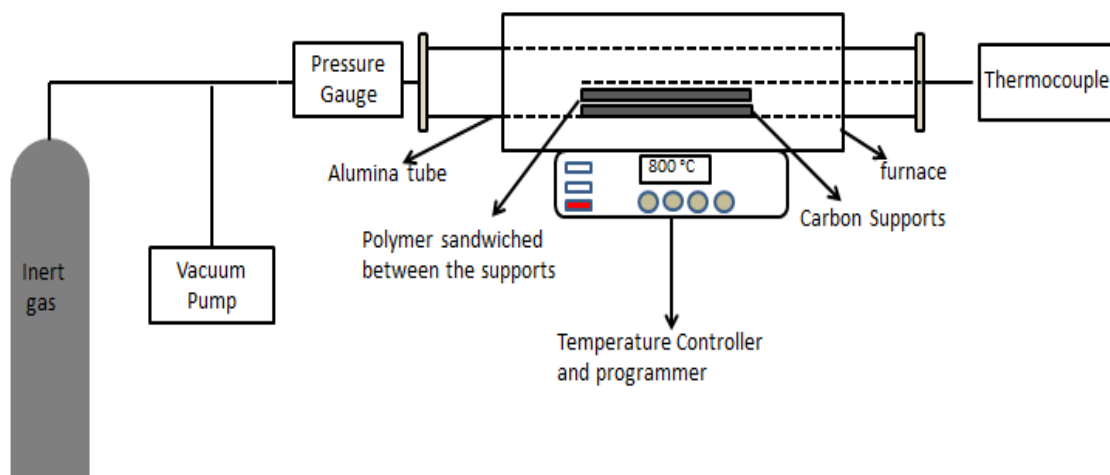


Figure 14 Schematic of Pyrolysis Setup

Once the setup is ready, vacuum is created inside the tube (up to a pressure -1 bar) using an external vacuum pump. The furnace is programmed to be heated up to a pyrolysis temperature 800 °C at a heating rate of 10 °C/min and held for 1 hour. The vacuum is

monitored using the vacuum gauge throughout the experiment and is maintained as -1 bar using the vacuum pump. The temperature is monitored using the external thermo-meter so as to avoid any time lag in temperature measurement of the sample. The furnace is allowed to cool down gradually to room temperature and the samples were removed. The polymer precursors carbonized completely can be seen in Figure 15.



**Figure 15** Polymer Precursors After Pyrolysis

### **3.4 PERMEATION SET-UP**

A time lag apparatus is built to measure the permeability of the pyrolyzed membranes according to the literature published elsewhere [101, 102]. The setup consists of a permeation cell which holds the membranes. The membrane in the cell is supported by a filter paper and a stainless steel sieve to give the membrane enough strength to withstand higher pressures. After placing the membrane in the cell a rubber gasket and O-ring was used to seal the cell from air leakage and the cell is closed using the bolts. The effective area of the membrane after placing the membrane was  $2.54\text{cm}^2$ . Both sides of the cells were provided with a vacuum supply to degas (remove any gas) the membrane.

A vacuum pump is used to degas the membranes and an additional vacuum reservoir is used to provide the vacuum while degassing the polymer for a long time. The feed gas is supplied from a gas cylinder. A digital pressure gauge cum controller is used at the feed side, which can read as well as control the pressure (up to a set point). The operating temperature and feed pressure were room temperature and 2atm, respectively. A small volume is used to collect the gases permeated through the membrane. A digital pressure gauge is attached to the permeation volume to measure the increasing pressure of the permeate gas. These two pressure gauges connected to a data acquisition system through USB ports which is connected to a PC. The data is recorded using flow vision software which records the data at sampling rate of one data per second. The variation of Upstream pressure (feed pressure) and downstream pressure (permeate side) along with the time were recorded. The complete setup can be visualized by the Figure 16.

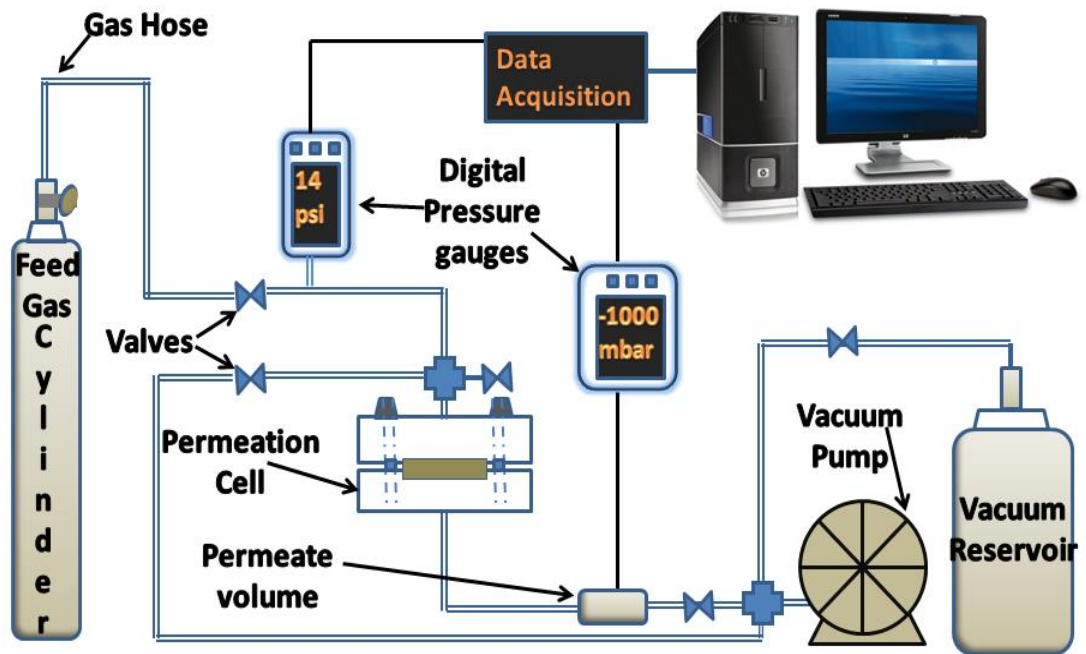


Figure 16 Schematic of Permeation Setup

After the pyrolysis, the pyrolyzed samples (self-supporting carbon molecular sieves) were placed in the permeation cell and vacuum is applied at both the ends with vacuum pump. Soon after the vacuum level is raised in the vacuum reservoir, the pump is disconnected. The membrane is held in the vacuum for 3-5 hours to make sure that any trapped gas in the membrane and cell is removed. Then feed is given to the upstream of the membrane and allowed to permeate downstream. The gas transport properties are calculated as in section 3.5.

### **3.5 PERMEATION MEASUREMENT**

Time lag method is widely used in studying the permeation of pure gas as well as gas mixtures in polymeric/inorganic membranes. The permeation properties (at both transient and steady state) of the system can be derived from the pressure-time response curves (at the downstream or upstream), as shown in Figure 17. In general, the transient mass transfer property (diffusion coefficient) is related to the time lag intercept while the steady state permeation flux can be derived from the slope [102]. Subject to different assumptions and boundary conditions, the time lag analysis also represents an excellent mathematical interpretation of a real physical process and is a powerful tool for characterizing membrane structure.

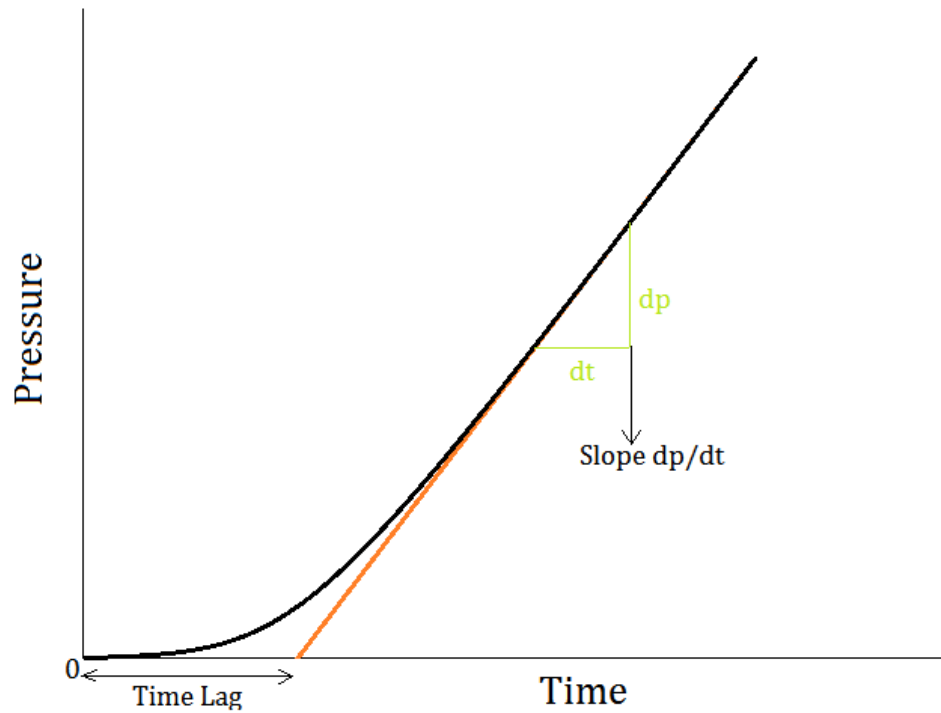


Figure 17 Pressure vs Time Response of an Ideal Time Lag Experiment

### 3.5.1 PERMEABILITY (P)

As discussed above the data is collected in a software and pressure vs time plots were plotted to obtain the slope  $\frac{dp}{dt}$  of the curve. The temperature is measured with a thermometer and the thickness of the membrane is measured with an electronic micrometer. The permeability of the gas in barrers is calculated using the formula [103, 104].

$$P = 22414 \cdot 10^{10} \frac{V}{R \cdot T} \cdot \frac{1}{A} \cdot \frac{l}{(p_1 - p_2)} \cdot \left( \frac{dp}{dt} \right) \quad (4.1)$$

The units are in barrers. [one Barrer =  $10^{-10} \cdot \frac{\text{cm}^3 \text{ (STP)} \cdot \text{cm}}{\text{cm}^2 \cdot \text{cmHg} \cdot \text{sec}}$  ]

Where,  $P$  is the permeability (in barrers);  $V$  is the volume of the downstream chamber (in  $\text{cm}^3$ );  $T$  signifies the temperature (in K);  $R$  is the gas constant ( $6236.56 \frac{\text{cm}^3 \cdot \text{cmHg}}{\text{mol} \cdot \text{K}}$ );  $A$  denotes the effective area of the membrane (in  $\text{cm}^2$ ),  $l$  is the membrane thickness (in cm);  $p_1$  is the feed pressure (in mbar);  $p_2$  is the permeate pressure (in mbar);  $\frac{dp}{dt}$  signifies the slope of the permeability vs time graph ( $\frac{\text{mbar}}{\text{sec}}$ ).

### 3.5.2 DIFFUSIVITY (D)

From the same Pressure vs time graph, the X-intercept of the graph is calculated which is also known as time lag. The time lag is the initial amount of the time taken by the gas to permeate from the membrane and to achieve a steady state. After obtaining the time lag the diffusivity can be calculated as,

$$D = \frac{l^2}{6\theta} \quad (4.2)$$

Where,  $D$  is the diffusivity (in  $\text{cm}^2 \cdot \text{s}^{-1}$ );  $l$  is the membrane thickness (in cm) and;  $\theta$  is the time lag (in sec).

### 3.5.3 SOLUBILITY (S)

Permeability is the product of diffusivity and solubility. Therefore, after obtaining the permeability and diffusivity, solubility can be calculated using the following equation

$$S = \frac{P}{D} \quad (4.3)$$

Where, S is the solubility (in  $\frac{\text{cm}^3 \text{ (STP)}}{\text{cm}^3 \cdot \text{cmHg}}$ ); P is the permeability (in barrers); D is the diffusivity (in  $\text{cm}^2 \cdot \text{s}^{-1}$ ).

### 3.5.4 SELECTIVITY ( $\alpha$ )

The ideal gas selectivity ( $\alpha$ ), also known as separation factor is the ratio of single permeability of any two gases [105]. Selectivity is the ratio of the permeabilities. After obtaining the permeabilities of oxygen and nitrogen, selectivity can be calculated as

$$\alpha_{ideal} \left( \frac{O_2}{N_2} \right) = \frac{P_{O_2}}{P_{N_2}} \quad (4.4)$$

## 3.6 CHARACTERIZATION METHODS

### 3.6.1 Thermo Gravimetric Analysis

Weight loss during pyrolysis is carried out using SDT Q 600 which features highly reliable horizontal dual balance mechanism and supports both TGA and DSC measurements. As the TGA system can withstand small pressure the inert purge is provided at a flowrate of 50 ml/min. TGA is done in inert gas environments such as Nitrogen, Argon and Helium etc., with a heating rate of 10 °C/min up to 1200 °C.

### **3.6.2 Scanning Electron Microscopy**

Scanning electron microscope (SEM) analysis are conducted using JEOL-JSM-6460LV. The pyrolyzed membranes were deposited on an aluminum holder with aid of a double sided copper tape. To improve the electric conductivity, the sample is coated with gold particles using Ion Sputter JFC-1100. The coated sample is then transferred in to JEOL Scanning Electron Microscope to examine the surface morphology of the sample. The SEM analysis is done using a Secondary electron image detector at room temperature and at a voltage of 5 kV.

### **3.6.3 X-Ray Diffraction**

X-Ray diffraction analysis was performed using BRUKER D8 ADVANCED. The samples were placed on a glass support and adhered to a holder using an adhesive. The measurement is taken between  $2^{\circ}$  to  $60^{\circ}$  with a step increment of  $0.02^{\circ}$  at room temperature.

### **3.6.4 Fourier Transforms Infrared Spectroscopy**

To detect the functional groups present in the membranes FTIR spectra is recorded on BRUKER VERTEX-70 spectrometer over the wave range of  $400\text{cm}^{-1}$  to  $4000\text{cm}^{-1}$ . The samples were placed in a film holder and the IR absorbance spectra is recorded with 16 sample scans and a resolution of  $4\text{ cm}^{-1}$ . Before recording the spectra an equal number of background scans were run to reduce the atmospheric peaks (like  $\text{CO}_2$ ,  $\text{H}_2\text{O}$  etc.. which absorbs IR radiation).

## CHAPTER 4

### RESULTS AND DISCUSSIONS

#### 4.1 TIME LAG ANALYSIS

After the data collection, pressure versus time graphs were plotted in order to obtain the slope ( $dp/dt$ ) and the time lag ( $\theta$ ). Leakage slope is obtained by keeping an impermeable film in the permeation cell and plotting the pressure raise in the permeate cell with respect to time. To get the accurate readings, the leakage slope is subtracted from the raw data. The steady state is reached in both permeation experiments of  $O_2$ ,  $N_2$  and it was observed that  $O_2$  permeated faster than the  $N_2$ . The pressure vs time plots for  $O_2$  and  $N_2$  permeation through CMS membrane (Table 3 entry 2) are given Figure 18. Nitrogen permeated in 950 seconds whereas oxygen permeated in 140 seconds to cause a pressure raise of 100 mbar.

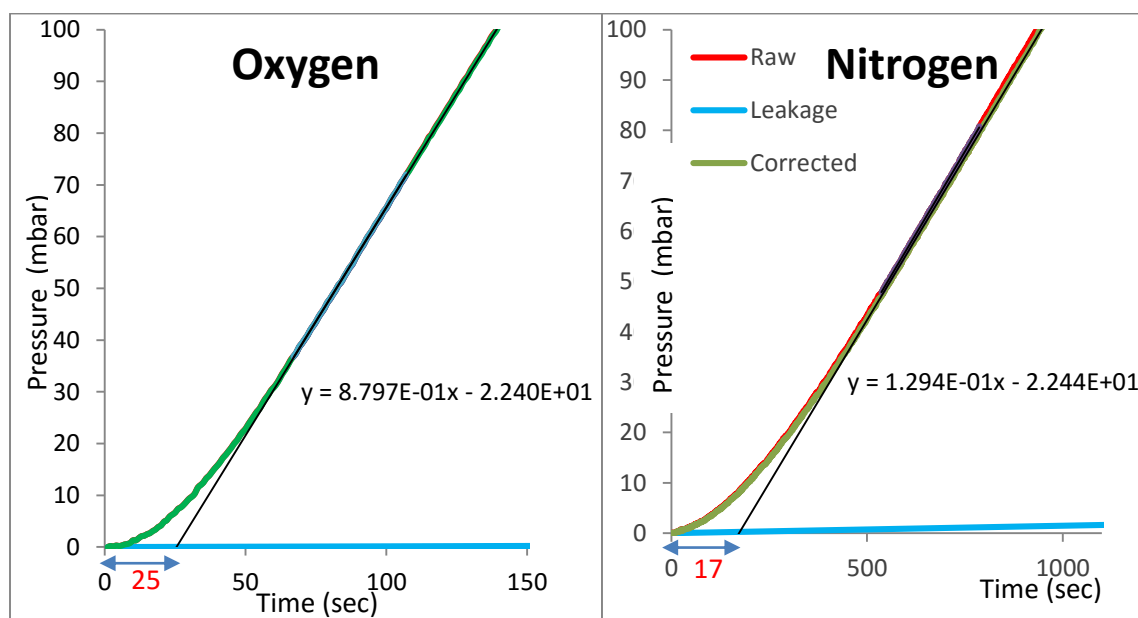


Figure 18 Pressure vs Time Plots for Oxygen and Nitrogen Permeation

## 4.2 GAS TRANSPORT PROPERTIES

### 4.2.1 CMS Derived from Different Kapton Films

Four types of Kapton films of same thickness (1 mil) were pyrolyzed in vacuum at 800 °C for one hour, the obtained CMS membranes found to have different permeabilities in a range of 0.32 barrers 25.88 barrers. These films can be categorized as very low, low, medium and high permeability samples (i.e VLP, LP, MP, HP respectively). The permeation properties of these CMS membranes are given in Table 4.

**Table 4 Permeation Properties of CMSM Derived from Different Kapton Films**

Sample name	Permeant gas	Permeability Barrers	Diffusivity $\left(\frac{\text{cm}^2}{\text{sec}}\right)$	Solubility $\left(\frac{\text{cm}^3 \text{ (STP)}}{\text{cm}^3 \cdot \text{cmHg.}}\right)$	Selectivity $\text{O}_2/\text{N}_2$
CMS-VLP	Oxygen	0.32	1.02E-09	3.09E-02	16.23
	Nitrogen	0.02	4.05E-10	4.80E-03	
CMS-LP	Oxygen	2.40	7.97E-09	3.01E-02	3.28
	Nitrogen	0.73	1.43E-09	5.11E-02	
CMS-MP	Oxygen	4.65	9.72E-09	4.79E-02	4.67
	Nitrogen	1.00	1.58E-09	6.32E-02	
CMS-HP	Oxygen	25.88	4.09E-08	6.33E-02	6.80
	Nitrogen	3.81	6.01E-09	6.34E-02	

The difference in the permeabilities can be attributed to various bonds present in the low permeability samples as discussed in the FTIR results. Figure 19 shows the FTIR

spectrum of four different Kapton films of same thickness, a clear difference can be seen b/w the KP-HP and other 3 low permeability samples (KP-VLP, KP-LP and KP-MP refer section 3.2 for abbreviations). All the films have O-H bond at  $3750\text{ cm}^{-1}$  except KP-LP. The polymer films KP-LP and KP-MP have aromatic C-H bond around  $680\text{ cm}^{-1}$  and KP-HP has N-H stretch in the range  $3600\text{ cm}^{-1} - 3700\text{ cm}^{-1}$ . Apart from these differences they have some similarities, the films have peak around  $1780\text{ cm}^{-1}$  shows characteristic of C=O imide stretching, the peaks at  $1617\text{ cm}^{-1}$  and  $1645\text{ cm}^{-1}$  are due to the aromatic C=C group. A sharp peak at  $3085\text{ cm}^{-1}$  signifies the C-H bond whereas a broad peak around  $1090\text{ cm}^{-1}$  signifies the presence of C-O-C structure in the polyimide.

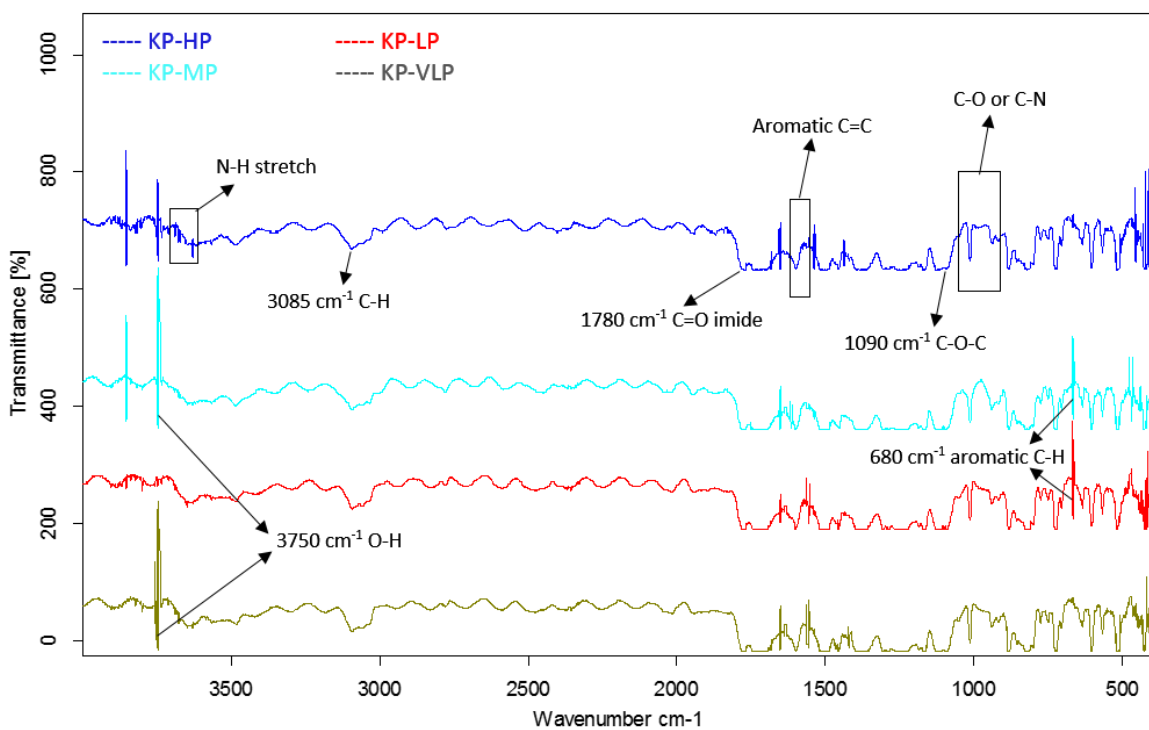
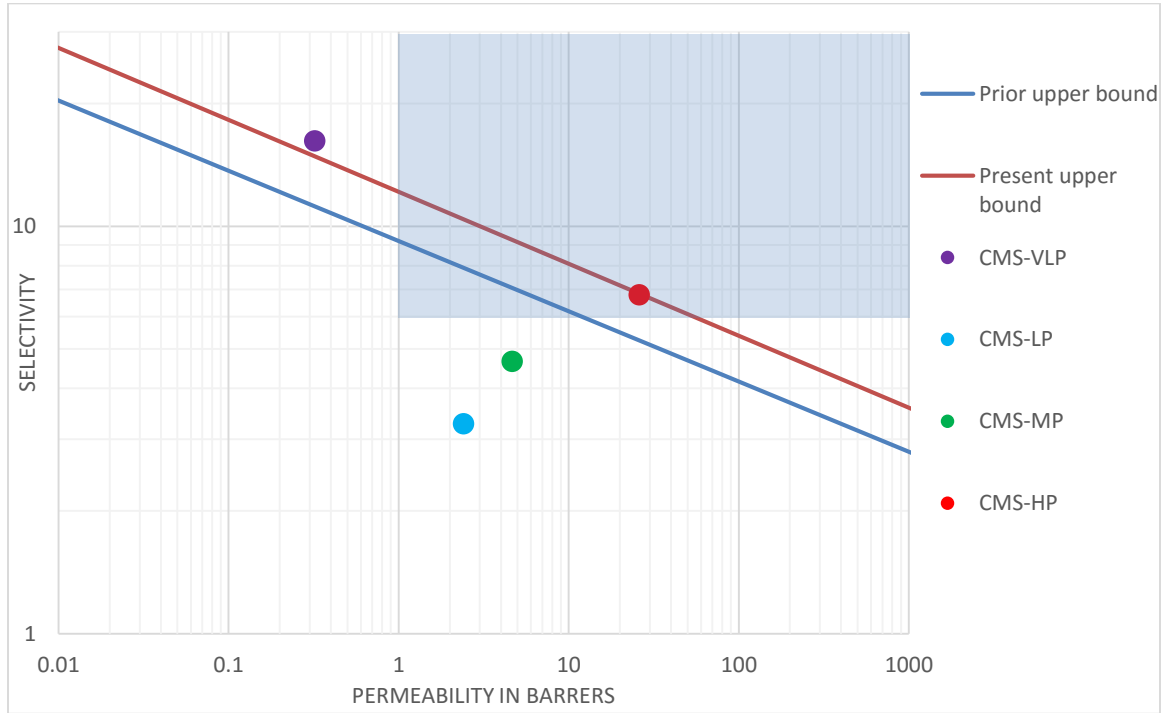


Figure 19 FTIR of Different Kapton Films

To be commercially attractive a membrane should have permeability greater than one with selectivity above six [106]. The permeation properties of table 3 are plotted on Robeson's plot as can be seen in Figure 20.



**Figure 20 Permeation Properties of CMSM Derived From Different Kapton Films.**

The permeabilities of the membranes CMS-LP and CMS-MP are in the commercially attractive range (>1 barrer) but their selectivities are not (<6). The selectivity of CMS-VLP is attractive but the permeability is very less. So, among these samples CMS-HP has been chosen for further treatments as both the permeability and selectivities of this sample are in the acceptable range (i.e permeability greater than one barrer and selectivity greater than 6) [106].

## 4.2.2 Varying Pyrolysis Parameters

### 4.2.2.1 Pyrolysis Environment

Pyrolysis is done in various atmospheres such as argon, helium, hydrogen and vacuum. TGA is a useful tool to find the weight loss of a material as a function of temperature. The polymer film was cut in to small pieces and placed in a small aluminum pan. Figure 21 shows the TGA thermo-gram of Kapton® polyimide. When the Kapton film is pyrolyzed under air (Oxidative environment), the membrane is completely lost at 650 °C which indicates the necessity of regulating the oxidative environment and providing the inert atmosphere during the pyrolysis. When air is replaced with inert atmosphere (Argon) the weight loss is decreased measurably from 100% to 50% weight loss. It is clear from the thermos-gram that Kapton is thermally stable in the 360 °C–410 °C range without any degradation. This result is in good agreement with the reported value of Chong et al [77].

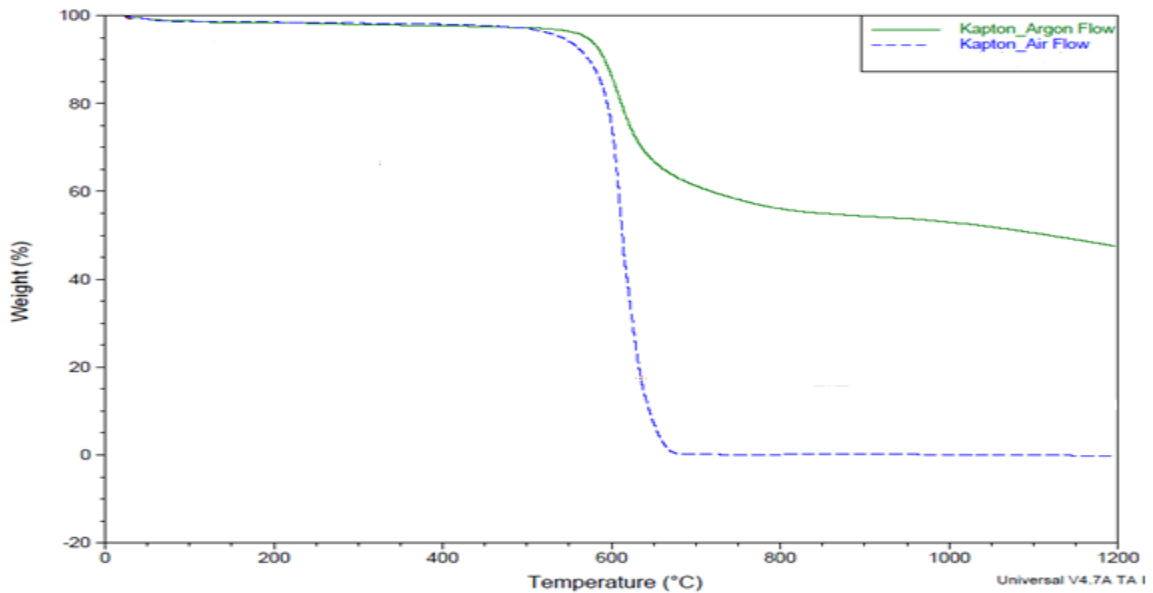


Figure 21 TGA Thermograms of Kapton® polyimide

The CMS samples pyrolyzed in vacuum have high permeability. The samples pyrolyzed in helium atmosphere have high O<sub>2</sub>/N<sub>2</sub> selectivity (8.17) but with less permeability (6.17 barrers). On the other hand, The CMS membranes pyrolyzed in vacuum atmosphere possess high permeability (25.88 barrers) with reasonable selectivity (6.8) as can be seen in Table 5 entry 1 .These results are in good agreement with the literature [80]. The study showed that the activation energy of degradation decreases significantly as the pressure of the inert pyrolysis atmosphere increases, thereby indicating possible differences in reaction mechanisms. During the vacuum pyrolysis the volatile byproducts reacted with the membrane by forming a more porous structure which improved the permeability when compared to the inert gas pyrolysis where the byproducts are removed.

**Table 5 Permeation Properties of CMSM Derived by Changing Pyrolysis Environment**

Pyrolysis environment	Permeant gas	Permeability Barrers	Diffusivity ( $\frac{\text{cm}^2}{\text{sec}}$ )	Solubility ( $\frac{\text{cm}^3 \text{ (STP)}}{\text{cm}^3 \cdot \text{cmHg.}}$ )	Selectivity O <sub>2</sub> /N <sub>2</sub>
Vacuum	Oxygen	25.88	4.09E-08	6.33E-02	6.80
	Nitrogen	3.81	6.01E-09	6.34E-02	
Argon	Oxygen	5.15	1.55E-08	3.31E-02	5.17
	Nitrogen	0.996	1.97E-09	5.07E-02	
Helium	Oxygen	6.15	1.41E-08	4.37E-02	8.17
	Nitrogen	0.75	2.02E-09	3.72E-02	
Hydrogen	Oxygen	12.70	2.26E-08	5.61E-02	6.13
	Nitrogen	2.07	4.63E-09	4.48E-02	

The data in the Table 5 is represented on Robeson's plot as can be seen in Figure 22. The membranes pyrolyzed under vacuum have better permeability and selectivity combinations. Therefore, vacuum is selected as pyrolysis environment.

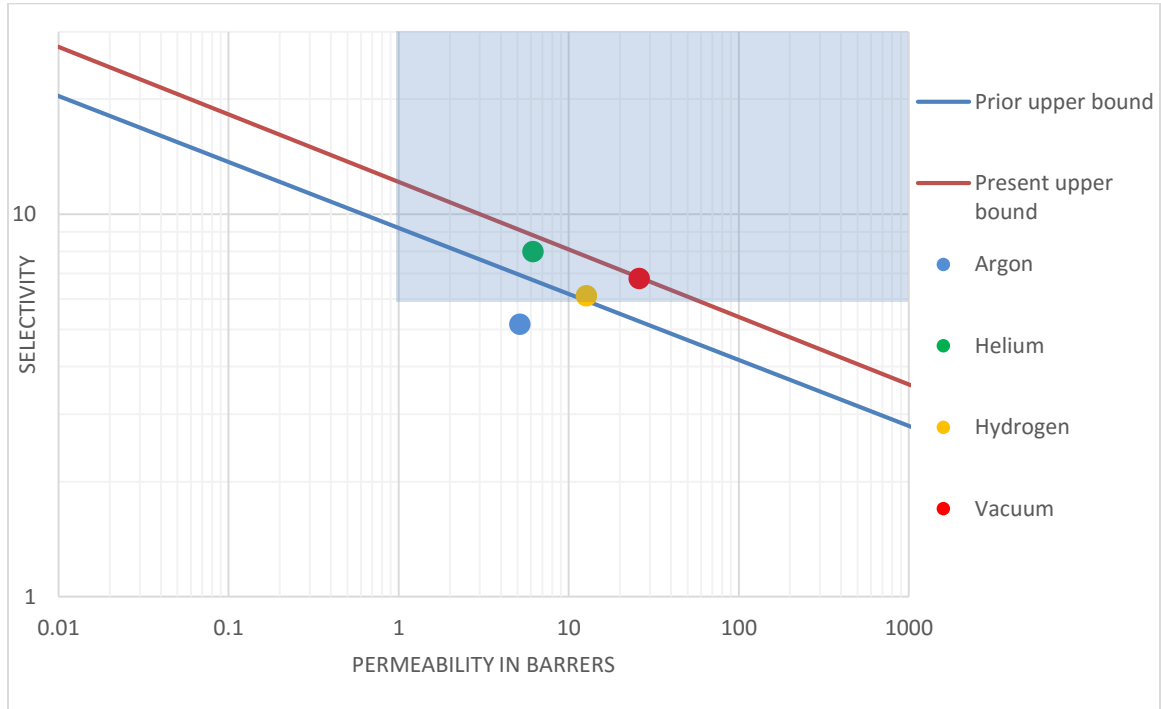


Figure 22 Permeation Properties of CMSM Derived by Varying Pyrolysis Atmosphere

#### 4.2.2.2 Pyrolysis Temperature

In order to optimize the pyrolysis temperature and obtain acceptable perm-selectivity combination, pyrolysis is done at three different temperatures 600 °C, 700 °C and 800 °C. Increasing the pyrolysis temperature lead to decrease in the permeability. As the temperature increased from 600 °C to 700 °C the permeability decreased by 40% with 80% increase in the selectivity. Similarly, when the temperature is increased from 700 °C to 800 °C the selectivity increased by 6% as can be seen in Table 6. The Data in Table 6

is represented on Robeson's plot as can be seen in Figure 23. The membranes pyrolyzed at 800 °C have better perm-selectivities when compared to other membranes.

**Table 6 Permeation Properties of CMSM Derived by Changing Pyrolysis Temperature**

Temperature In °C	Permeant Gas	Permeability Barrers	Diffusivity ( $\frac{\text{cm}^2}{\text{sec}}$ )	Solubility ( $\frac{\text{cm}^3 \text{ (STP)}}{\text{cm}^3 \cdot \text{cmHg.}}$ )	Selectivity O <sub>2</sub> /N <sub>2</sub>
600	Oxygen	70.39	2.23E-07	3.16E-02	3.57
	Nitrogen	19.71	5.96E-08	3.31E-02	
700	Oxygen	42.57	7.18E-08	5.93E-02	6.45
	Nitrogen	6.60	1.10E-08	5.98E-02	
800	Oxygen	25.88	4.09E-08	6.33E-02	6.80
	Nitrogen	3.81	6.01E-09	6.34E-02	

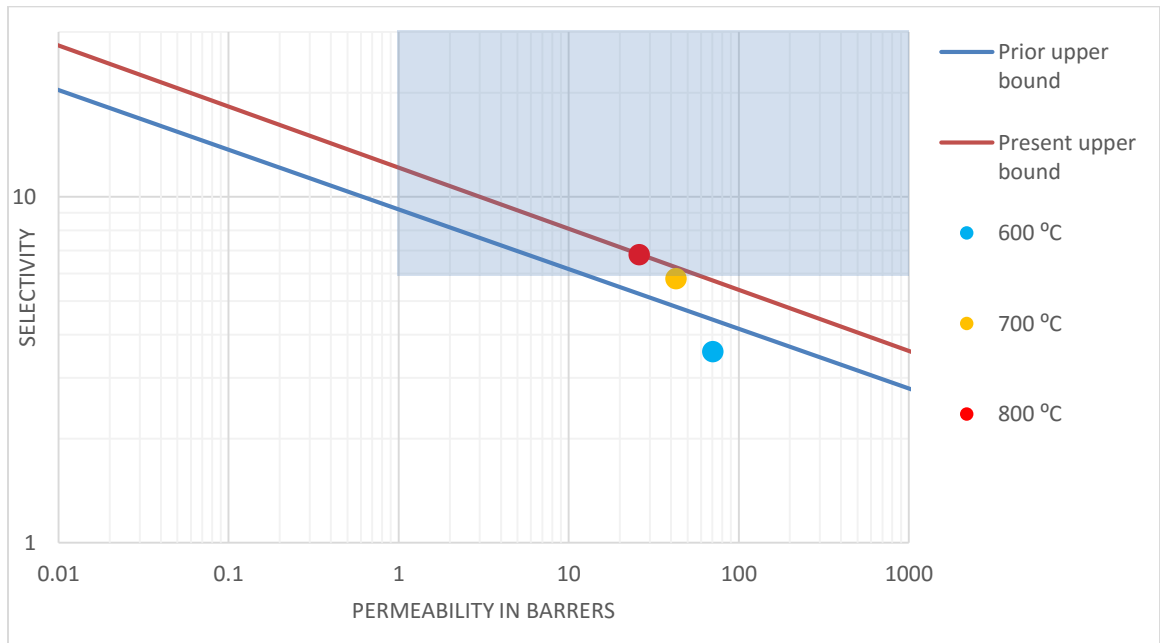


**Figure 23 Permeation Properties of CMSM Derived by Changing Pyrolysis Temperature**

### 4.2.3 Pre Treated Samples

#### 4.2.3.1 CMS Derived from Pre Heated Kapton Films

The polyimide is preheated at four different preheating temperatures (i.e 250 °C, 300 °C, 350 °C and 400 °C respectively). Black carbon spots appeared when the film is heated beyond 400 °C. The preheated samples found to have high permeabilities and low selectivities when compared to the untreated sample. In the early stages, increasing the preheating temperature (i.e up to 350 °C) improved the permeability of the resultant membranes, as can be seen in Table 7.

**Table 7 Permeation Properties of CMSM Derived from Preheated Kapton Films**

Pre Heated up to temperature	Permeant gas	Permeability (P) Barrers	Diffusivity ( $\frac{\text{cm}^2}{\text{sec}}$ )	Solubility ( $\frac{\text{cm}^3 \text{ (STP)}}{\text{cm}^3 \cdot \text{cmHg.}}$ )	Selectivity O <sub>2</sub> /N <sub>2</sub>
-	Oxygen	25.88	4.09E-08	6.33E-02	6.80
	Nitrogen	3.81	6.01E-09	6.34E-02	
250 °C	Oxygen	27.07	7.43E-08	3.64E-02	3.55
	Nitrogen	7.62	1.35E-08	5.66E-02	
300 °C	Oxygen	44.65	6.56E-08	6.80E-02	3.60
	Nitrogen	12.42	2.37E-08	5.24E-02	
350 °C	Oxygen	49.80	6.96E-08	7.15E-02	4.53
	Nitrogen	10.99	3.20E-08	3.44E-02	
400 °C	Oxygen	28.66	5.51E-08	5.20E-02	5.20
	Nitrogen	5.51	1.27E-08	4.32E-02	

But, when the preheating temperature increased up to 400 °C the permeability decreased. Whereas the selectivity is keeps on increasing for all the preheating temperatures. Similar results of increase in the permeability with the temperature are reported by Centeno and Fuertes [57]. The data in Table 7 is plotted on Robeson’s plot as in Figure 24.

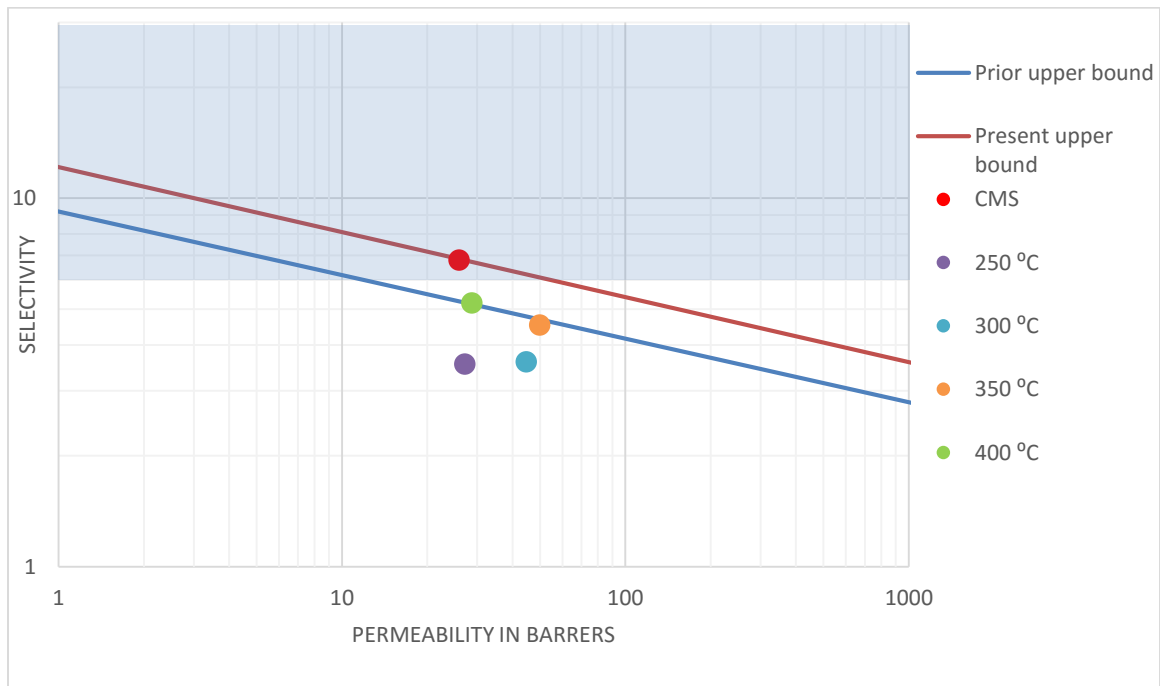


**Figure 24** Permeation Properties of CMSM Membranes Derived from Preheated Kapton Films.

#### 4.2.3.2 CMS derived from chemically treated Kapton films

The Kapton films are pre-treated with N-methyl-2-pyrrolidone (NMP) prior to the pyrolysis. The Kapton films were cut in the form of circular discs and pretreated with NMP in three different ways. Firstly, the polyimide is kept in NMP solution for 24 hours and then cleaned with tissue paper. Secondly, the polyimide is washed with water after 24 hours NMP treatment. Lastly, the polyimide is washed with water after 12 hour NMP

treatment, then after drying again kept in NMP for 12 more hours and washed with water. All the above membranes were pyrolyzed at 800 °C in vacuum atmosphere with one hour holding time.

**Table 8 Permeation Properties of CMSM Derived from Chemically Treated Kapton Film**

Chemical	Permeant gas	Permeability (P) Barrers	Diffusivity $\left(\frac{\text{cm}^2}{\text{sec}}\right)$	Solubility $\left(\frac{\text{cm}^3 \text{ (STP)}}{\text{cm}^3 \cdot \text{cmHg.}}\right)$	Selectivity O <sub>2</sub> /N <sub>2</sub>
-	Oxygen	25.88	4.09E-08	6.33E-02	6.80
	Nitrogen	3.81	6.01E-09	6.34E-02	
NMP (Cleaned with Paper)	Oxygen	22.33	2.97E-08	7.53E-02	10.81
	Nitrogen	2.07	4.53E-09	4.56E-02	
NMP (water treated at end)	Oxygen	23.79	3.02E-08	7.88E-02	7.15
	Nitrogen	3.33	6.74E-09	4.94E-02	
NMP (IWT)	Oxygen	26.78	3.92E-08	6.83E-02	8.87
	Nitrogen	3.02	5.47E-09	5.52E-02	
HF	Oxygen	27.12	4.24E-08	6.40E-02	6.57
	Nitrogen	4.13	5.72E-09	7.22E-02	
HCL	Oxygen	22.20	3.99E-08	5.56E-02	4.00
	Nitrogen	5.55	1.69E-08	3.28E-02	
NH <sub>4</sub> CL	Oxygen	14.83	2.32E-08	6.39E-02	6.17
	Nitrogen	2.40	4.34E-09	5.53E-02	
Methanol	Oxygen	29.92	5.27E-08	5.67E-02	6.00
	Nitrogen	4.98	9.68E-09	5.15E-02	

Among the CMS membranes, the first method of NMP treatment is found useful in increasing the selectivity by 59% with a slight loss of permeability as in entry 2 Table 8 . The third method of NMP treatment improved permeability and selectivity by 3.5% and 30.44% respectively. The polyimide is also pre-treated with different acids (HF, HCl and NH<sub>4</sub>Cl) but the separation properties of the resultant CMS membranes did not improve. Whereas methanol treatment of the polymeric precursor prior to the pyrolysis was able to improve the permeability of the resultant membrane with slight loss of selectivity as shown in Figure 25. The results are discussed in section 4.2.5.

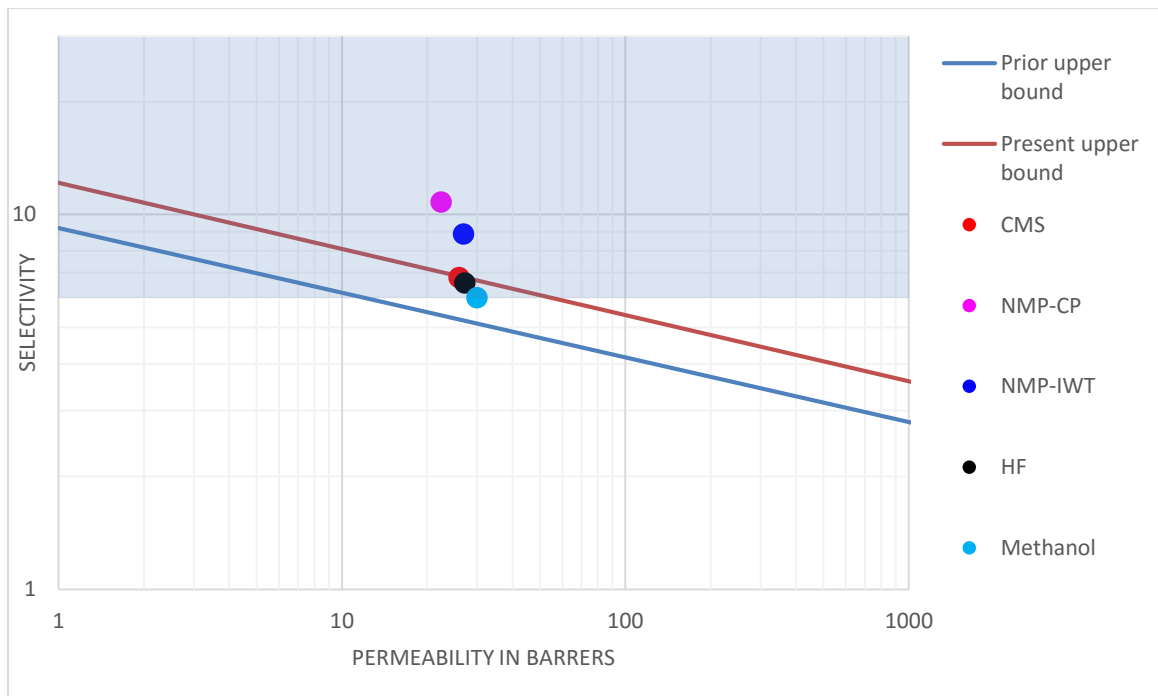


**Figure 25** Permeation Properties of CMSM Derived from Chemically Pretreated Samples.

#### 4.2.4 Post Heat Treated CMS Samples

The carbon molecular sieve is post heated at four different temperatures (i.e 325 °C, 350 °C, 375 °C and 400 °C respectively). The post-heated samples found to have less permeabilities and low selectivities when compared to the untreated sample. As the post heat treatment temperature increased both the permeability and selectivity started deteriorating. As can be seen in the Table 9 and Figure 26. These results are discussed in section 4.2.5.

**Table 9 Permeation Properties of Post Heat Treated CMS Samples**

Post heat treatment temperature	Gas used	Permeability Barrers	Diffusivity $\left(\frac{\text{cm}^2}{\text{sec}}\right)$	Solubility $\left(\frac{\text{cm}^3 \text{ (STP)}}{\text{cm}^3 \cdot \text{cmHg.}}\right)$	Selectivity O <sub>2</sub> /N <sub>2</sub>
-	Oxygen	25.88	4.09E-08	6.33E-02	6.80
	Nitrogen	3.81	6.01E-09	6.34E-02	
325 °C	Oxygen	21.83	3.68E-08	5.93E-02	3.72
	Nitrogen	5.87	1.03E-08	5.72E-02	
350 °C	Oxygen	10.45	2.33E-08	4.49E-02	3.91
	Nitrogen	2.68	6.91E-09	3.87E-02	
375 °C	Oxygen	5.20	1.81E-08	2.87E-02	3.13
	Nitrogen	1.66	4.11E-09	4.04E-02	
400 °C	Oxygen	1.71	6.26E-09	2.73E-02	2.62
	Nitrogen	0.65	2.23E-09	2.92E-02	

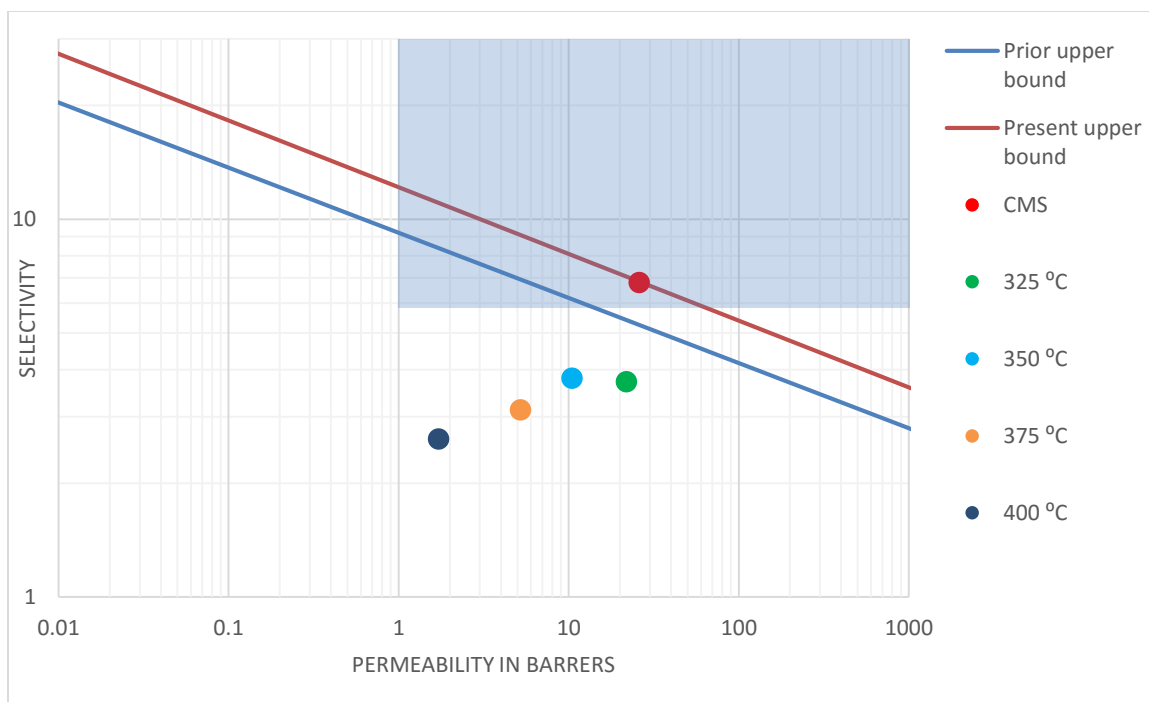


**Figure 26 Permeation Properties of Post Heat Treated CMSM.**

In CMS membranes both large pores and ultramicropores are believed to coexist. The large pores enhance the adsorption whereas the ultramicropores imparts selectivity to the membrane. The ultramicropores are speculated to be created at “kinks” in the carbon sheet or from the edge of a carbon sheet as can be seen in Figure 27.

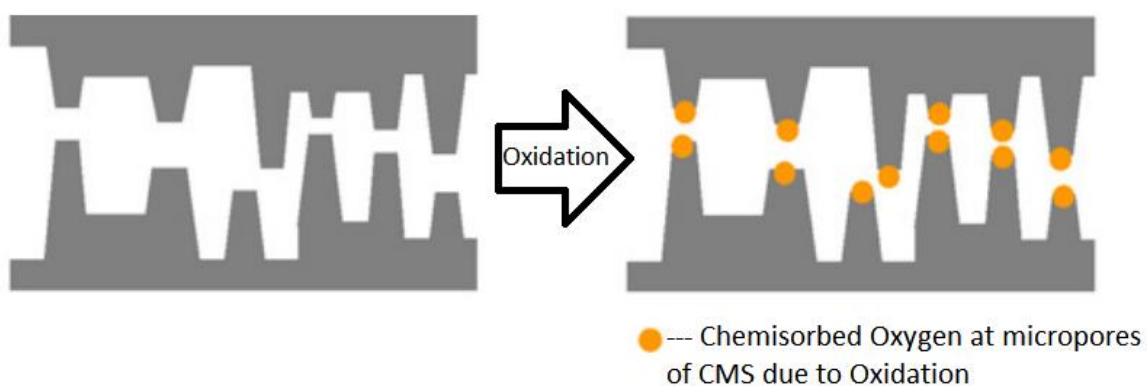


**Figure 27 Oxygen Doping During the Oxidation of CMS membrane.**

These sites are more susceptible to oxidation than other sites due to presence of more reactive unpaired electrons [107]. It is postulated that, at first the oxygen reacts with the membrane surface then diffuses into the membrane and reacts with the ultramicropores due to chemisorption and formation of carbonyls [108, 109]. During the Post oxidation stable oxides such as CO, CO<sub>2</sub> and surface oxides are produced by oxygen molecules[79]. Increasing the post heat treatment temperature lead to decrease in both permeability and selectivity, possibly suggesting that oxygen may have filled most of the “active” sites of ultramicropores, reducing both selectivity and permeability.

#### **4.2.5 Optimized Samples**

The raw Kapton film which lead to CMS-HP has a very low permeability i.e 0.029 barrers and a selectivity (O<sub>2</sub>/N<sub>2</sub>) of 6.81. After the pyrolysis the permeability of the membrane increased to 26 barrers (almost 1000 times) while retaining the same selectivity (Table 10). For further improvement of the permeability and/or selectivity, the precursor polymer has been pretreated either by heat or chemicals.

Firstly, Kapton samples were heated to 350 °C in an air-furnace for one hour. The CMS membrane obtained after this heat treatment has almost doubled the permeability (from 25.8 barrers to 49.8 barrers) but with loss of selectivity (from 6.8 to 4.53) this confirms the enlargement of pores on the CMS membrane.

**Table 10 Permeation Properties of Kapton Before and After Pyrolysis with Various Pre and Post Treatments.**

Sample name	Permeant gas	Permeability Barrers	Diffusivity ( $\frac{\text{cm}^2}{\text{sec}}$ )	Solubility $\frac{\text{cm}^3 \text{ (STP)}}{\text{cm}^3 \cdot \text{cmHg.}}$	Selectivity O <sub>2</sub> /N <sub>2</sub>
KP	Oxygen	0.029	7.56E-10	3.80E-03	6.81
	Nitrogen	0.004	-	-	
CMS	Oxygen	25.88	4.09E-08	6.33E-02	6.8
	Nitrogen	3.81	6.01E-09	6.34E-02	
CMS-HT-BP	Oxygen	49.8	6.96E-08	7.15E-02	4.53
	Nitrogen	10.99	3.20E-08	3.44E-02	
CMS-HT-AP	Oxygen	10.45	2.33E-08	4.49E-02	3.91
	Nitrogen	2.68	6.91E-09	3.87E-02	
CMS-NMP-CP	oxygen	22.33	2.97E-08	7.53E-02	10.81
	nitrogen	2.07	4.53E-09	4.56E-02	
CMS-NMP-IWT	oxygen	26.78	3.92E-08	6.83E-02	8.87
	nitrogen	3.02	5.47E-09	5.52E-02	

The oxidation pretreatment allows the polymeric precursor to retain its form and structure during pyrolysis as a result of the formation of crosslinks in the polymer that increase its thermal stability [57]. Similar results were found in this study, the heat treated sample developed aromatic C-H bond around 680  $\text{cm}^{-1}$  and also the number of peaks which represents the C=O bond increased as depicted in Figure 28. Centeno and Fuertes [57] heat treated a phenolic resin in air (i.e oxidative environment) in a temperature range

from 150 °C-300 °C for 2 hours. The permeation rate of the resultant CMS membrane was found to improve significantly. Yamamoto et al [110] prepared BPDA-ODA/DAT co-polyimide membrane on a porous alumina support and heat treated it in air up to 400 °C for one hour prior to the pyrolysis. The CMS membranes thus prepared were found to have more permeance than the membranes obtained by untreated polyimide. The above results (i.e. permeability enhancement) are in good agreement with this study.

Secondly, Kapton samples were soaked in NMP solvent for 24 hours prior to pyrolysis. The obtained CMS membrane has shown an improvement in selectivity (10.8) with a small loss of permeability (i.e from 25.88 barrers to 22.3 barrers) (Table 10). NMP treatment of Kapton film increased number of C-H and C-N bonds when compared to the raw Kapton film, which increased the carbon yield and a more selective structure is formed after the pyrolysis. NMP is strongly bound to the carboxylic acid group in Kapton film due to the electronegativity of the oxygen atom. The carboxylic NMP helps to prevent the reverse reaction that would otherwise degrade the Kapton film and regenerate the original monomers. Fortunately, the precursor and NMP have C=O in their chemical structure, so it's difficult to confirm the presence of NMP using C=O stretching band at  $1671\text{ cm}^{-1}$ . However, the presence of NMP can be confirmed by C-H and C-N bonds at bands  $980\text{ cm}^{-1}$  and  $1050\text{ cm}^{-1}$  respectively. N-H groups Kapton film reacted with the C=O groups in NMP leads to an isotropic film with a smooth surface morphology.

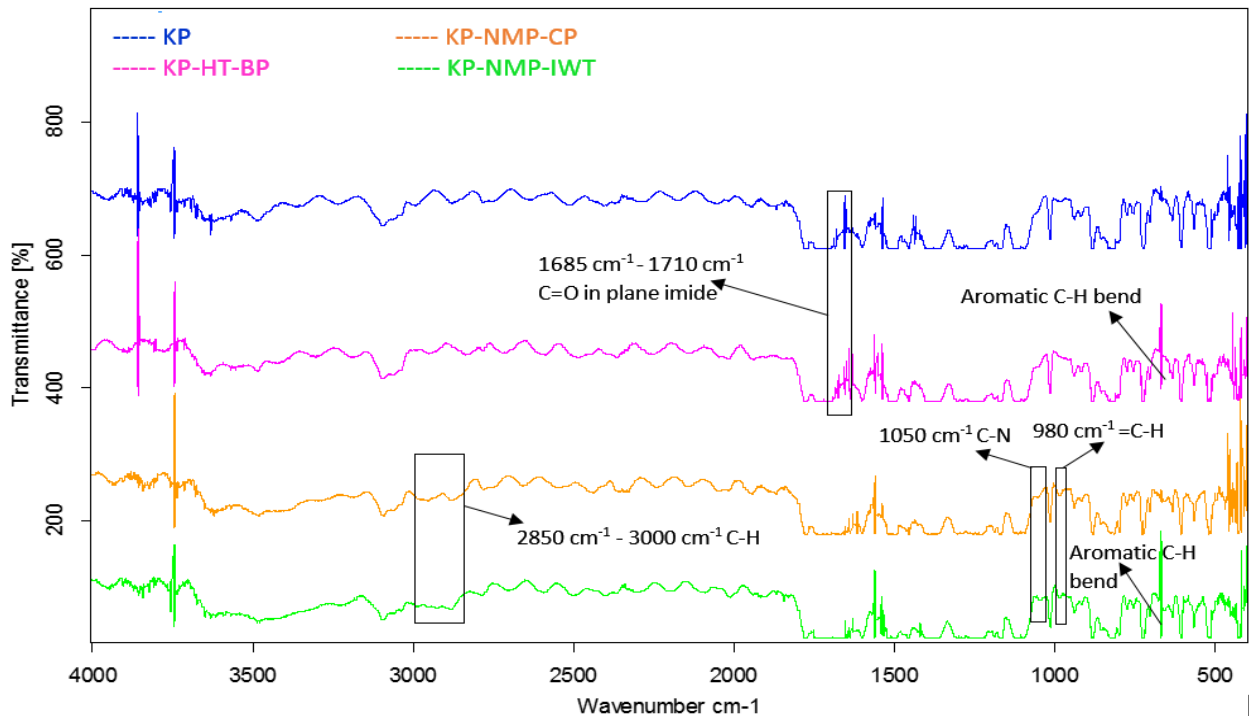


Figure 28 FTIR of Raw and Pretreated Kapton Films

Figure 28 shows the difference between the FTIR spectra of neat and pre-treated samples. The NMP treated polymer films (KP-NMP-CP and KP-NMP-IWT) don't have a peak around  $3800\text{ cm}^{-1}$  which is present in the neat polymer and also these samples developed new bonds such as C-H and C-N after the treatment. Similar effect of increase in the selectivity was reported elsewhere. Schindler and Maier [111] used an aqueous hydrazine solution to pre-treat acrylonitrile prior to the pyrolysis which enabled tight pore size distribution and adjusted the pore sizes. Tin et al. [26, 56] immersed polyimide Matrimid 5218 in methanol solution for various time periods and observed that the pretreatment improved the selectivity of the CMS membrane. This pretreatment enhanced the mobility of the polymer chains and their structural arrangement to form a micropores, which is

confirmed by high carbon yield of the resultant CMS membrane when compared to the untreated membrane. Deacetylation of cellulose acetate precursor prior to the pyrolysis step was useful to get a CMS membrane with optimum performance as reported by He et al [112].

Thirdly, before pyrolysis, Kapton samples were soaked in NMP solvent for 12 hours, washed with ionized water, air-dried, and then soaked again in NMP for 12 hours. The resulting CMS membrane from this chemical treatment showed better permeability (26.8) and selectivity (8.9) than that of membranes without treatment (Table 10). As the precursors washed with water after every 12 hours during the pretreatment, the NMP content in the precursor decreased up to a critical level during the pyrolysis and anti-plasticization took place after certain temperature. Which improved both the permselectivities of the membrane. Increasing the soak time up to 36 hours and 48 hours lead to formation of fragile membranes with less permeability. The permeability decreased drastically from 26.8 barrers to 16.92 barrers and 5.47 barrers respectively. Combining both the pre-treatments, that is soaking the polymer in NMP for one day and then heating it in air-furnace up to 350 °C prior to the pyrolysis was also not able to improve any of the permeation properties (i.e permeability of oxygen 20.23 barrers and selectivity 4.36).

In addition to the above pre-treatment of the precursor Kapton film, post-heat-treatment of the CMS membranes were performed. In this study, CMS were subjected to heat in air-furnace at 350 °C for one hour. It is observed that this treatment of the CMS membrane has resulted in decreasing both permeability and selectivity by 60% and 43%, respectively (Table 10). The reason for decrease in the permeability might be attributed to

the pore blockage due to excessive oxygen exposure during the post oxidation heat treatment. In general, post oxidation heat treatment improves the permeability due to increase in the micro pore volume and pore size distribution. As an example, the heat treatment of CMS membranes derived from BPDA-pp'ODA polyimide at 300 °C in oxidative environment improved the gas permeation due to enlargement of the pores as reported by Hayashi [89] and Kusakabe [90] et al.

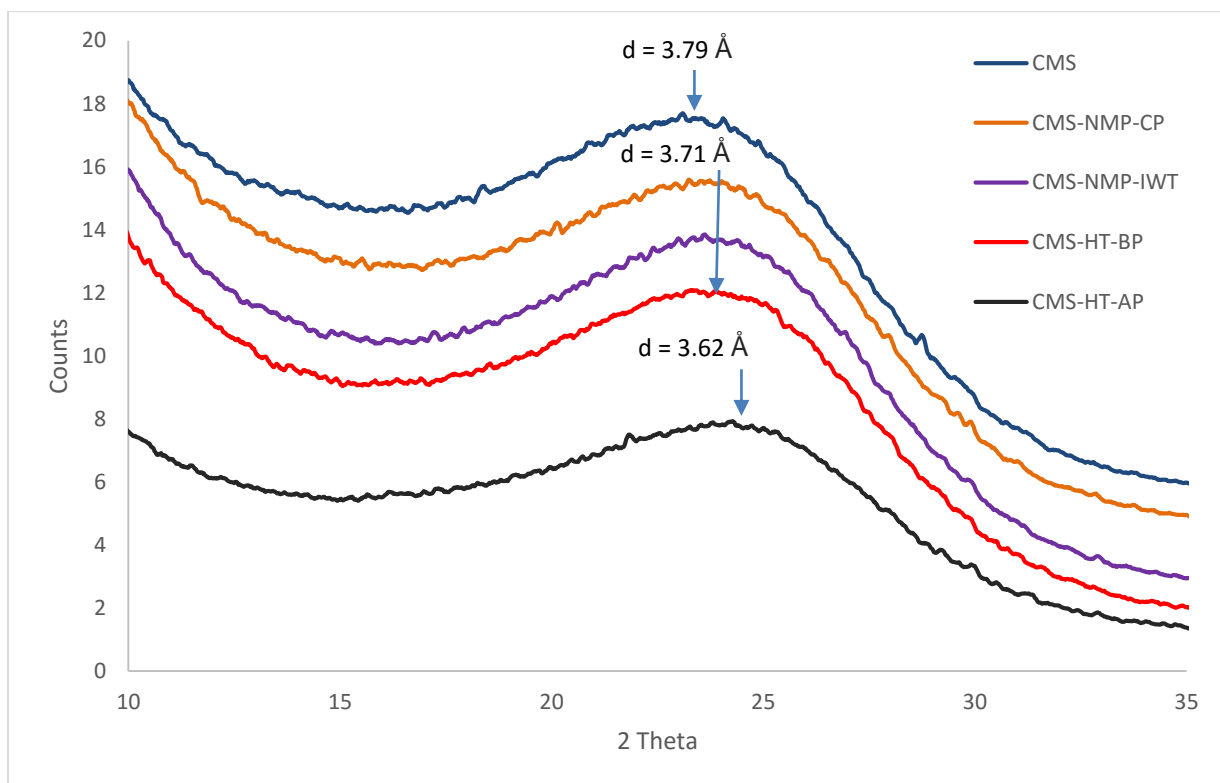


**Figure 29 XRD Spectra of Kapton**

XRD was used to find inter molecular spacing of the pyrolyzed membranes. Figure 29 shows the XRD patterns of the CMS membranes prepared by fore mentioned procedures. The intermolecular spacing can be calculated by using Braggs law, every membrane has a broad hump around  $2\theta=24^\circ$  which represents the amorphous graphitic structure. This

result is in good agreement with the value reported by Kaburagi et al [113] and Su et al [114]. As reported by Sing et al [34] the slit like nanopores with smaller spacing (3.8 Å) can decrease the rotational degrees of freedom of N<sub>2</sub> thereby increasing the selectivity O<sub>2</sub>/N<sub>2</sub>. According to Figure 29, all membranes have small inter-molecular spacing in the range of 3.62 Å to 3.79 Å. It should be noted that the free space between carbon molecules can be determined, by subtracting the size of the carbon molecule (1.34 Å) [115], to be in the range 2.28 Å to 2.45 Å. In this range neither oxygen nor nitrogen can pass through this space because of their larger sizes (where diameter of the oxygen and nitrogen is 3.46 Å and 3.64 Å respectively). On the other hand, the change in the permeability can be explained by considering the intensity of the XRD curves at lower angles (i.e from 2θ range 10°-15°). The XRD curves of high permeability samples (CMS, CMS-NMP and CMS-HT-BP) are higher than that of CMS-HT-AP.

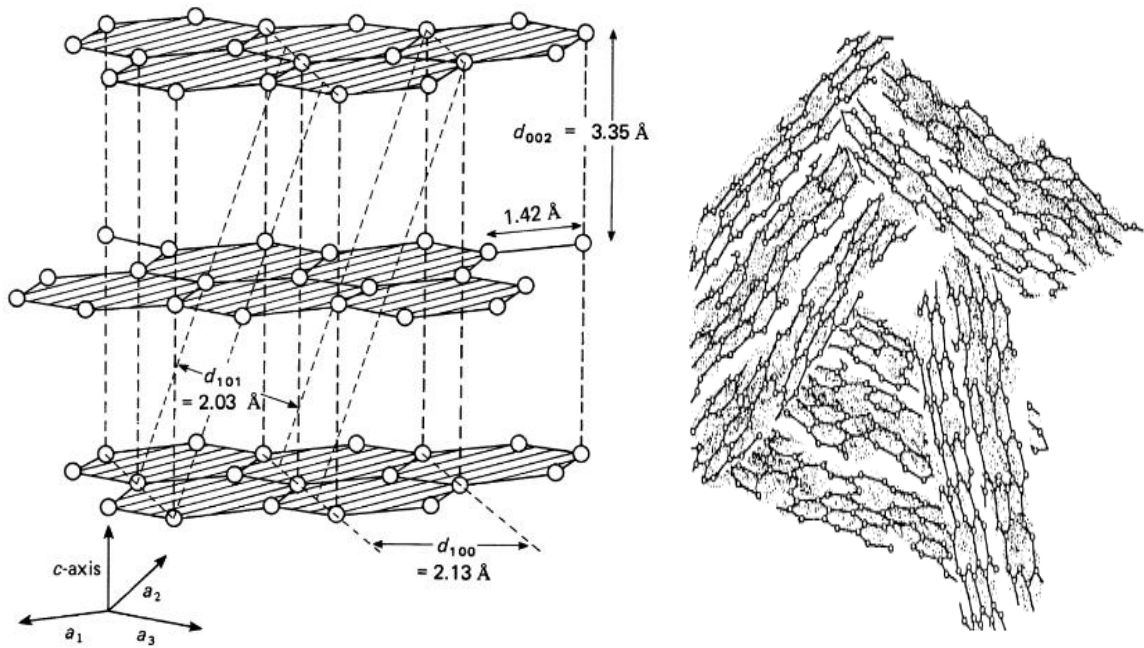
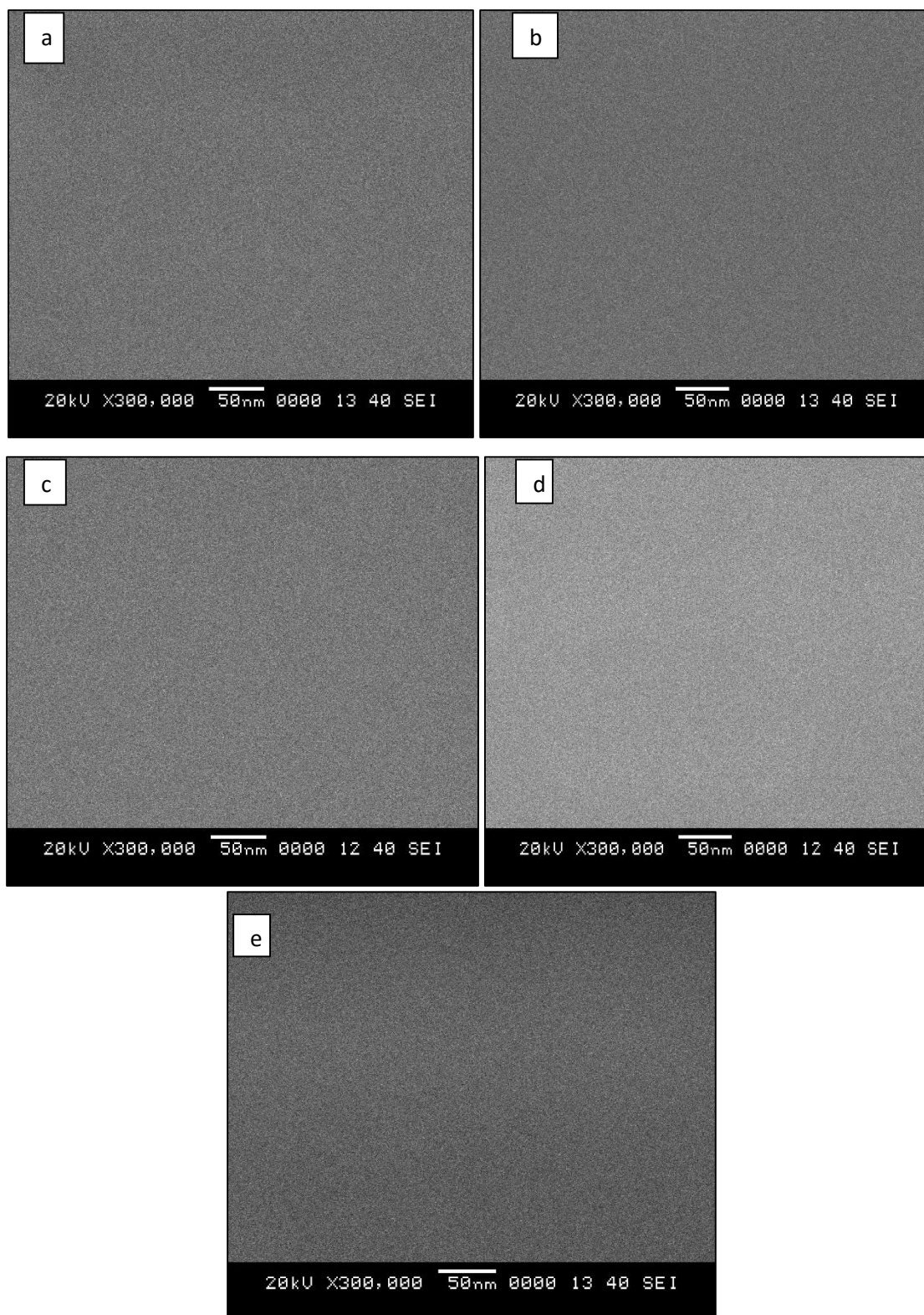


Figure 30 Atomic Structure of (a) Perfect Graphite (b) Turbo Static graphite .



**Figure 31** Surface Topologies of CMS membranes: (a) CMS; (b) CMS-HT-AP; (c) CMS-HT-BP; (d) CMS-NMP-CP; (e) CMS-NMP-IWT

The structures of these membranes are examined by SEM. For a better understanding of the pore characteristics, the SEM images were taken at high magnification (i.e 300k). The surface topologies of all the CMS membranes are similar as can be seen in the Figure 31. They don't have any large pores or cracks which affects the permeation properties and thereby reducing the membrane performance. Therefore, the difference in the permeation properties is mostly due to the change in the internal structure of the membrane.

The data in the Table 10 is plotted on the Robeson's upper bound for a better comparison. The values reported in the literature also plotted for a comparison as can be seen in the Figure 32.

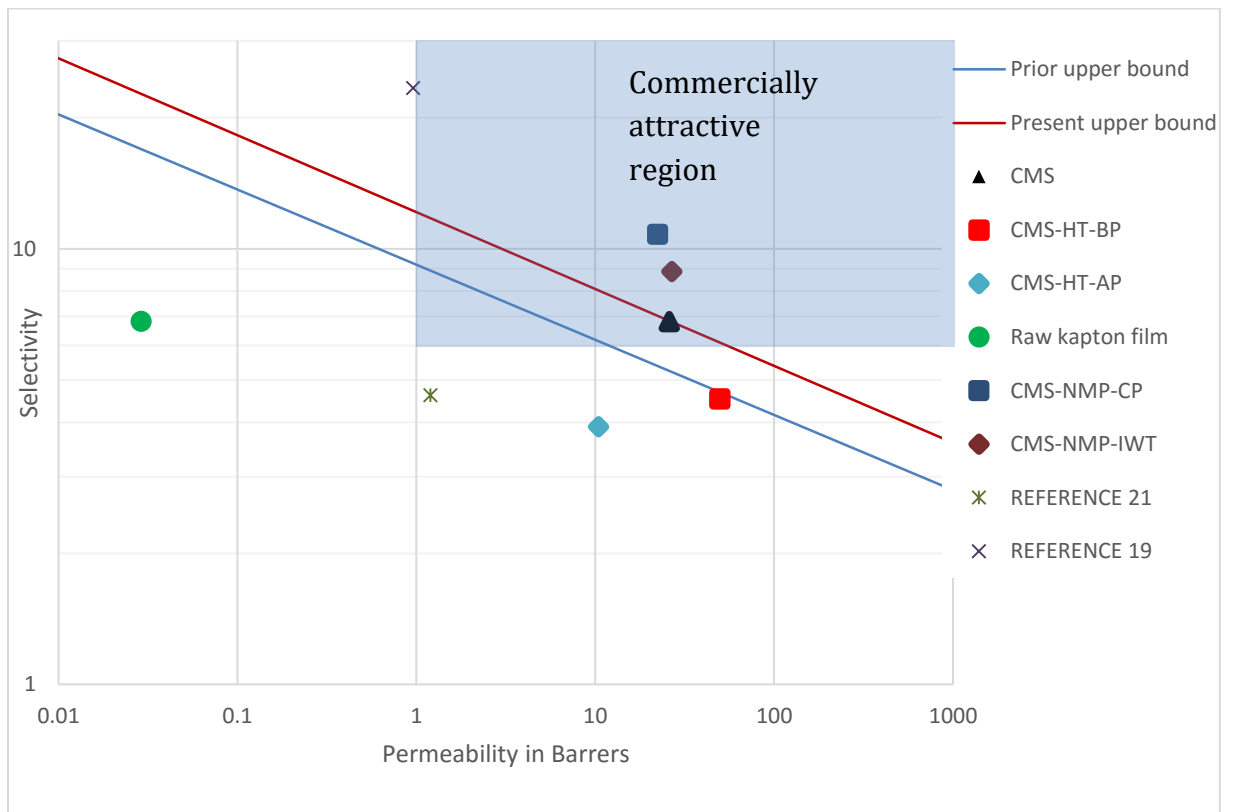


**Figure 32 Representation of Permeation Properties on Robeson's Plot**

The separation performance of the precursor Kapton sample is located below the upper bounds. After pyrolysis, the obtained result of CMS membrane is located exactly on the upper bound of Robeson-2008 plot, in the commercially attractive region. The separation performance of the membranes prepared by NMP treatment surpassed the upper bound due to their high selectivities whereas oxidation heat treated samples were not able to cross it.

## CHAPTER 5

### CONCLUSIONS

Self-supported flat sheet carbon molecular sieve membranes had been prepared by pyrolyzing the Kapton polyimide under various pyrolysis conditions and the separation performance was seen to surpass the Robeson's upper bound line for oxygen nitrogen separation. Among the pyrolysis parameters, vacuum is optimized as pyrolysis atmosphere and a temperature of 800°C as final pyrolysis temperature. The optimized pyrolysis parameters were used for the preparation of all the subsequent pre and post treated samples. The following conclusions can be drawn from this study.

- ❖ Single gas permeation tests revealed that all the membranes exhibited molecular sieving properties. The polyimide film pyrolyzed without any treatment had an oxygen permeability of 25.9 barrers and a selectivity ( $O_2/N_2$ ) of 6.8.
- ❖ Pre heating the polymer prior to the pyrolysis was optimized at a temperature of 350 °C for 1 hour which almost doubled the oxygen permeability (49.9 barrers) of the resultant CMS membrane. The FTIR
- ❖ Pretreating the polymer precursor with N-methyl pyrrolidone for 24 hours prior to the pyrolysis improved the selectivity of  $O_2/N_2$  from 6.8 to 10.81 without much loss of oxygen permeability (22.3 barrers) when compared to untreated membrane (25.88 barrers). The increase in the selectivity is due to plasticization effect of NMP retained in the precursor after the pre-treatment.

- ❖ Intermediate water washing during NMP treatment after 12 hours enhanced both the permeability and selectivity when compared to the untreated membrane. Thus treating the Kapton polyimide with NMP prior to the pyrolysis has been proven as an effective technique to enhance the permeation properties of the derived CMS membrane.
  
- ❖ Heating the carbon molecular sieve membrane in oxidative environment lead to decrease in both permeability and selectivity, suggesting that the oxygen chemisorbed at the ultramicropores.
  
- ❖ XRD and FTIR analysis of the CMS membranes gave support to the decomposition of the imide molecules and formation of turbo static graphitic structure after the pyrolysis.
  
- ❖ SEM analysis confirmed that all the CMS membranes thus formed don't have any large pores or cracks which severely effects the membrane performance.

## **CHAPTER 6**

### **RECOMMENDATIONS FOR FUTURE WORK**

In this study, the research objectives are achieved and significant contributions have been made in many aspects of CMS membranes for oxygen/nitrogen separation. However, numerous opportunities are available for further research, this section contains recommendations for future work in the field of CMS membranes.

#### **PREPARING SUPPORTED CMS MEMBRANES**

In this study, self-supported CMS membranes were synthesized which are very brittle and difficult to handle. These membranes are more susceptible to breakage while placing the membrane in the permeation cell and creating the pressure difference across the membrane. To improve the strength of these CMS membranes, the polymer precursor can be casted on a support and then subjected to pyrolysis. In order to successfully fabricate a supported CMS membrane, the support material must be chosen so that, during the pyrolysis it will shrink similar to the polymer casted on it. Choosing a material with low carbon yield as the substrate will improve the permeation flux and casting a high carbon yield material on the substrate will impart selectivity to the resultant membrane. In a recent study, CMS membranes supported on porous tubular supports with high O<sub>2</sub>/N<sub>2</sub> selectivity (15.4) prepared by Lee et al [116].

## **PREPARING CMS MMM MEMBRANES**

As discussed earlier, polymers possess good flexibility whereas CMS membranes are known for their ability to separate gases. To combine these two properties, polymer matrix can be incorporated with CMS particles to fabricate mixed matrix membranes which possess good permeation properties and flexible as well. There are hardly any publications reporting CMS MMS. The research made by Vu et al [117] is on among them, in which they prepared CMS from pyrolysis of a polyimide (Matrimid) at pyrolysis temperature 800 °C, and then ball milled the CMS to get fine particles up to 2microns. These particles then incorporated into two different polymers matrimid® 5218 and Ultem® 1000 to form flat sheet mixed matrix membranes for gas separation. The resulted MMM generated molecular sieving channels and pores which are high size selective for air separation.

## **VARYING OPERATIONAL PARAMETERS**

In this study, feed gas is supplied at 1 atm pressure and permeate side is kept at vacuum. But, in realistic applications these parameters may vary according to the need. Therefore, the membranes are to be prepared to sustain in practical air separation applications such as high pressure feed streams, in cryogenic atmosphere, in high pressure difference across the membrane etc.

The operating temperature is also an important factor which determines the permeation rate. In this study, the membranes were tested at room temperature. Varying the temperature will control the activation energy of diffusion and hence influence the

permeation of the gases through the membrane. So, the permeation cell can be equipped with a heating element and a temperature controller to check the effect of operating temperature on the permeation properties. In a recent study by Yoshimune et al [118], selectivity is reported to be decreased with increase in the feed pressure and temperature for CO<sub>2</sub>/CH<sub>4</sub> separation.

Single gas permeation tests were performed on the CMS membranes, whereas in practical applications mixed gas will be supplied as feed. So, further investigation can be done by performing mixed gas permeation tests.

## REFERENCES

1. Baker, R.W., *Future Directions of Membrane Gas Separation Technology*. Industrial & Engineering Chemistry Research, 2002. **41**(6): p. 1393-1411.
2. Yampolskii, Y., *Polymeric Gas Separation Membranes*. Macromolecules, 2012. **45**(8): p. 3298-3311.
3. Mannan, H.A., et al., *Recent applications of polymer blends in gas separation membranes*. Chemical Engineering & Technology, 2013. **36**(11): p. 1838-1846.
4. Rufford, T.E., et al., *The removal of CO<sub>2</sub> and N<sub>2</sub> from natural gas: A review of conventional and emerging process technologies*. Journal of Petroleum Science and Engineering, 2012. **94–95**(0): p. 123-154.
5. Rochelle, G.T., *Amine scrubbing for CO<sub>2</sub> capture*. Science, 2009. **325**(5948): p. 1652-1654.
6. Rezaei, F. and P. Webley, *Structured adsorbents in gas separation processes*. Separation and Purification Technology, 2010. **70**(3): p. 243-256.
7. Ferreira, D., et al., *Single-Stage Vacuum Pressure Swing Adsorption for Producing High-Purity Oxygen from Air*. Industrial & Engineering Chemistry Research, 2015. **54**(39): p. 9591-9604.
8. Eriksson, T. and Y. Kiros, *Temperature swing adsorption device for oxygen-enriched air*. Journal of Cleaner Production, 2014. **76**: p. 174-179.
9. Naheiri, T., et al., *Nitrogen and oxygen separation using vacuum swing adsorption*. 2013, Google Patents.

10. Burdyny, T. and H. Struchtrup, *Hybrid membrane/cryogenic separation of oxygen from air for use in the oxy-fuel process*. Energy, 2010. **35**(5): p. 1884-1897.
11. Allam, R.J., *Improved oxygen production technologies*. Energy Procedia, 2009. **1**(1): p. 461-470.
12. Wilcox, J., *Cryogenic Distillation and Air Separation*, in *Carbon Capture*. 2012, Springer New York. p. 219-229.
13. Fane, A.G., R. Wang, and Y. Jia, *Membrane Technology: Past, Present and Future*, in *Membrane and Desalination Technologies*, L. Wang, et al., Editors. 2011, Humana Press. p. 1-45.
14. Bernardo, P. and G. Clarizia, *30 Years of Membrane Technology for Gas Separation*. CHEMICAL ENGINEERING, 2013. **32**.
15. Maier, G., *Gas Separation with Polymer Membranes*. Angewandte Chemie International Edition, 1998. **37**(21): p. 2960-2974.
16. Robeson, L.M., *Polymer membranes for gas separation*. Current Opinion in Solid State and Materials Science, 1999. **4**(6): p. 549-552.
17. Abedini, R. and A. Nezhadmoghadam, *Application of membrane in gas separation processes: its suitability and mechanisms*. Petroleum & Coal, 2010. **52**(2): p. 69-80.
18. Sanders, D.F., et al., *Energy-efficient polymeric gas separation membranes for a sustainable future: A review*. Polymer, 2013. **54**(18): p. 4729-4761.

19. Baker, R.W. and B.T. Low, *Gas Separation Membrane Materials: A Perspective*. *Macromolecules*, 2014. **47**(20): p. 6999-7013.
20. Murphy, T.M., et al., *Physical aging of layered glassy polymer films via gas permeability tracking*. *Polymer*, 2011. **52**(26): p. 6117-6125.
21. Rowe, B.W., B.D. Freeman, and D.R. Paul, *Physical aging of ultrathin glassy polymer films tracked by gas permeability*. *Polymer*, 2009. **50**(23): p. 5565-5575.
22. Visser, T., N. Masetto, and M. Wessling, *Materials dependence of mixed gas plasticization behavior in asymmetric membranes*. *Journal of Membrane Science*, 2007. **306**(1-2): p. 16-28.
23. Wessling, M., et al., *Plasticization of gas separation membranes*. *Gas Separation & Purification*, 1991. **5**(4): p. 222-228.
24. Park, H.B., et al., *Relationship between chemical structure of aromatic polyimides and gas permeation properties of their carbon molecular sieve membranes*. *Journal of Membrane Science*, 2004. **229**(1-2): p. 117-127.
25. Kim, Y.K., et al., *The gas separation properties of carbon molecular sieve membranes derived from polyimides having carboxylic acid groups*. *Journal of Membrane Science*, 2004. **235**(1-2): p. 139-146.
26. Tin, P.S., et al., *Novel approaches to fabricate carbon molecular sieve membranes based on chemical modified and solvent treated polyimides*. *Microporous and Mesoporous Materials*, 2004. **73**(3): p. 151-160.

27. Julbe, A., *Chapter 6 Zeolite membranes — synthesis, characterization and application*, in *Studies in Surface Science and Catalysis*, H.v.B.A.C. Jiří Čejka and S. Ferdi, Editors. 2007, Elsevier. p. 181-219.
28. van de Graaf, J.M., et al., *Effect of Operating Conditions and Membrane Quality on the Separation Performance of Composite Silicalite-1 Membranes*. *Industrial & Engineering Chemistry Research*, 1998. **37**(10): p. 4071-4083.
29. Caro, J., et al., *Zeolite membranes – state of their development and perspective*. *Microporous and Mesoporous Materials*, 2000. **38**(1): p. 3-24.
30. Lin, Y.S., et al., *MICROPOROUS INORGANIC MEMBRANES*. *Separation & Purification Reviews*, 2002. **31**(2): p. 229-379.
31. Ismail, A.F. and L.I.B. David, *A review on the latest development of carbon membranes for gas separation*. *Journal of Membrane Science*, 2001. **193**(1): p. 1-18.
32. Robeson, L.M., *Correlation of separation factor versus permeability for polymeric membranes*. *Journal of Membrane Science*, 1991. **62**(2): p. 165-185.
33. Robeson, L.M., *The upper bound revisited*. *Journal of Membrane Science*, 2008. **320**(1–2): p. 390-400.
34. Singh, A. and W.J. Koros, *Significance of Entropic Selectivity for Advanced Gas Separation Membranes*. *Industrial & Engineering Chemistry Research*, 1996. **35**(4): p. 1231-1234.

35. Rungta, M., L. Xu, and W.J. Koros, *Carbon molecular sieve dense film membranes derived from Matrimid® for ethylene/ethane separation*. Carbon, 2012. **50**(4): p. 1488-1502.
36. Saufi, S.M. and A.F. Ismail, *Fabrication of carbon membranes for gas separation—a review*. Carbon, 2004. **42**(2): p. 241-259.
37. Barsema, J.N., et al., *Carbon molecular sieve membranes prepared from porous fiber precursor*. Journal of Membrane Science, 2002. **205**(1–2): p. 239-246.
38. Steel, K.M. and W.J. Koros, *Investigation of porosity of carbon materials and related effects on gas separation properties*. Carbon, 2003. **41**(2): p. 253-266.
39. Jung, C., et al., *Gas separation of pyrolyzed polymeric membranes: Effect of polymer precursor and pyrolysis conditions*. Macromolecular Research, 2007. **15**(6): p. 565-574.
40. Das, M., J.D. Perry, and W.J. Koros, *Effect of processing on carbon molecular sieve structure and performance*. Carbon, 2010. **48**(13): p. 3737-3749.
41. Belyaev, A.A., et al., *Membrane air separation for intensification of coal gasification process*. Fuel Processing Technology, 2003. **80**(2): p. 119-141.
42. Leo, A., S. Liu, and J.C.D.d. Costa, *Development of mixed conducting membranes for clean coal energy delivery*. International Journal of Greenhouse Gas Control, 2009. **3**(4): p. 357-367.
43. Budd, P.M. and N.B. McKeown, *Highly permeable polymers for gas separation membranes*. Polymer Chemistry, 2010. **1**(1): p. 63-68.

44. Nunes, S.P. and K.V. Peinemann, *Gas Separation with Membranes*, in *Membrane Technology*. 2001, Wiley-VCH Verlag GmbH. p. 39-67.
45. Park, H.B. and Y.M. Lee, *Polymeric Membrane Materials and Potential Use in Gas Separation*, in *Advanced Membrane Technology and Applications*. 2008, John Wiley & Sons, Inc. p. 633-669.
46. Lu, W., et al., *Porous Polymer Networks: Synthesis, Porosity, and Applications in Gas Storage/Separation*. *Chemistry of Materials*, 2010. **22**(21): p. 5964-5972.
47. Pandey, P. and R.S. Chauhan, *Membranes for gas separation*. *Progress in Polymer Science*, 2001. **26**(6): p. 853-893.
48. Gilron, J. and A. Soffer, *Knudsen diffusion in microporous carbon membranes with molecular sieving character*. *Journal of Membrane Science*, 2002. **209**(2): p. 339-352.
49. Carta, M., et al., *An Efficient Polymer Molecular Sieve for Membrane Gas Separations*. *Science*, 2013. **339**(6117): p. 303-307.
50. Barrer, R.M., *Diffusion in and through Solids*. 1941: CUP Archive.
51. Van Amerongen, G.J., *Influence of structure of elastomers on their permeability to gases*. *Journal of Polymer Science*, 1950. **5**(3): p. 307-332.
52. Soffer, A., et al., *Carbon membranes*. GB patent, 1989. **2207666**.
53. Kiyono, M., P.J. Williams, and W.J. Koros, *Effect of polymer precursors on carbon molecular sieve structure and separation performance properties*. *Carbon*, 2010. **48**(15): p. 4432-4441.

54. Low, B.T. and T.S. Chung, *Carbon molecular sieve membranes derived from pseudo-interpenetrating polymer networks for gas separation and carbon capture*. Carbon, 2011. **49**(6): p. 2104-2112.
55. Williams, P.J. and W.J. Koros, *Gas Separation by Carbon Membranes*, in *Advanced Membrane Technology and Applications*. 2008, John Wiley & Sons, Inc. p. 599-631.
56. Tin, P.S., T.-S. Chung, and A.J. Hill, *Advanced Fabrication of Carbon Molecular Sieve Membranes by Nonsolvent Pretreatment of Precursor Polymers*. Industrial & Engineering Chemistry Research, 2004. **43**(20): p. 6476-6483.
57. Centeno, T.A. and A.B. Fuertes, *Carbon molecular sieve membranes derived from a phenolic resin supported on porous ceramic tubes*. Separation and Purification Technology, 2001. **25**(1-3): p. 379-384.
58. Geiszler, V.C. and W.J. Koros, *Effects of polyimide pyrolysis conditions on carbon molecular sieve membrane properties*. Industrial and Engineering Chemistry Research, 1996. **35**(9): p. 2999-3003.
59. Suda, H. and K. Haraya, *Gas Permeation through Micropores of Carbon Molecular Sieve Membranes Derived from Kapton Polyimide*. The Journal of Physical Chemistry B, 1997. **101**(20): p. 3988-3994.
60. Xu, L., et al., *Physical aging in carbon molecular sieve membranes*. Carbon, 2014. **80**: p. 155-166.
61. Lagorsse, S., F.D. Magalhães, and A. Mendes, *Aging study of carbon molecular sieve membranes*. Journal of Membrane Science, 2008. **310**(1-2): p. 494-502.

62. HÄGg, M.-B., J.A. Lie, and A. LindbrÅThen, *Carbon Molecular Sieve Membranes*. Annals of the New York Academy of Sciences, 2003. **984**(1): p. 329-345.
63. Jones, C.W. and W.J. Koros, *Carbon molecular sieve gas separation membranes-II. Regeneration following organic exposure*. Carbon, 1994. **32**(8): p. 1427-1432.
64. Fuertes, A.B., D.M. Nevskaiia, and T.A. Centeno, *Carbon composite membranes from Matrimid® and Kapton® polyimides for gas separation*. Microporous and Mesoporous Materials, 1999. **33**(1-3): p. 115-125.
65. Hatori, H., et al., *Carbon molecular sieve films from polyimide*. Carbon, 1992. **30**(4): p. 719-720.
66. Acharya, M. and H.C. Foley, *Spray-coating of nanoporous carbon membranes for air separation*. Journal of Membrane Science, 1999. **161**(1-2): p. 1-5.
67. Shiflett, M.B. and H.C. Foley, *Reproducible production of nanoporous carbon membranes*. Carbon, 2001. **39**(9): p. 1421-1425.
68. Kita, H., et al., *Gas permselectivity of carbonized polypyrrolone membrane*. Chemical Communications, 1997(11): p. 1051-1052.
69. Singh-Ghosal, A. and W.J. Koros, *Air separation properties of flat sheet homogeneous pyrolytic carbon membranes*. Journal of Membrane Science, 2000. **174**(2): p. 177-188.
70. Barsema, J.N., et al., *Intermediate polymer to carbon gas separation membranes based on Matrimid PI*. Journal of Membrane Science, 2004. **238**(1-2): p. 93-102.

71. Xiao, Y., et al., *Effects of Brominating Matrimid Polyimide on the Physical and Gas Transport Properties of Derived Carbon Membranes*. *Macromolecules*, 2005. **38**(24): p. 10042-10049.
72. Steel, K.M. and W.J. Koros, *An investigation of the effects of pyrolysis parameters on gas separation properties of carbon materials*. *Carbon*, 2005. **43**(9): p. 1843-1856.
73. Kim, Y.K., H.B. Park, and Y.M. Lee, *Preparation and characterization of carbon molecular sieve membranes derived from BTDA–ODA polyimide and their gas separation properties*. *Journal of Membrane Science*, 2005. **255**(1–2): p. 265-273.
74. Fu, Y.-J., et al., *Development and characterization of micropores in carbon molecular sieve membrane for gas separation*. *Microporous and Mesoporous Materials*, 2011. **143**(1): p. 78-86.
75. Islam, M.N., et al., *Preparation and gas separation performance of flexible pyrolytic membranes by low-temperature pyrolysis of sulfonated polyimides*. *Journal of Membrane Science*, 2005. **261**(1–2): p. 17-26.
76. Hosseini, S.S., et al., *Enhancing the properties and gas separation performance of PBI–polyimides blend carbon molecular sieve membranes via optimization of the pyrolysis process*. *Separation and Purification Technology*, 2014. **122**(0): p. 278-289.
77. Lua, A.C. and J. Su, *Effects of carbonisation on pore evolution and gas permeation properties of carbon membranes from Kapton® polyimide*. *Carbon*, 2006. **44**(14): p. 2964-2972.

78. Anderson, C.J., et al., *Effect of pyrolysis temperature and operating temperature on the performance of nanoporous carbon membranes*. Journal of Membrane Science, 2008. **322**(1): p. 19-27.
79. Kiyono, M., P.J. Williams, and W.J. Koros, *Effect of pyrolysis atmosphere on separation performance of carbon molecular sieve membranes*. Journal of Membrane Science, 2010. **359**(1–2): p. 2-10.
80. Geiszler, V.C. and W.J. Koros, *Effects of Polyimide Pyrolysis Conditions on Carbon Molecular Sieve Membrane Properties*. Industrial & Engineering Chemistry Research, 1996. **35**(9): p. 2999-3003.
81. David, L.I.B. and A.F. Ismail, *Influence of the thermastabilization process and soak time during pyrolysis process on the polyacrylonitrile carbon membranes for O<sub>2</sub>/N<sub>2</sub> separation*. Journal of Membrane Science, 2003. **213**(1–2): p. 285-291.
82. Suda, H. and K. Haraya, *Gas permeation through micropores of carbon molecular sieve membranes derived from Kapton polyimide*. Journal of Physical Chemistry B, 1997. **101**(20): p. 3988-3994.
83. Lafyatis, D.S., J. Tung, and H.C. Foley, *Poly(furfuryl alcohol)-derived carbon molecular sieves: Dependence of adsorptive properties on carbonization temperature, time, and poly(ethylene glycol) additives*. Industrial and Engineering Chemistry Research, 1991. **30**(5): p. 865-873.
84. Campo, M.C., F.D. Magalhães, and A. Mendes, *Carbon molecular sieve membranes from cellophane paper*. Journal of Membrane Science, 2010. **350**(1–2): p. 180-188.

85. Shao, L., T.-S. Chung, and K.P. Pramoda, *The evolution of physicochemical and transport properties of 6FDA-durene toward carbon membranes; from polymer, intermediate to carbon*. *Microporous and Mesoporous Materials*, 2005. **84**(1–3): p. 59-68.
86. Centeno, T.A., J.L. Vilas, and A.B. Fuertes, *Effects of phenolic resin pyrolysis conditions on carbon membrane performance for gas separation*. *Journal of Membrane Science*, 2004. **228**(1): p. 45-54.
87. Fuertes, A.B., *Effect of air oxidation on gas separation properties of adsorption-selective carbon membranes*. *Carbon*, 2001. **39**(5): p. 697-706.
88. Lee, H.-C., et al., *Use of Steam Activation as a Post-treatment Technique in the Preparation of Carbon Molecular Sieve Membranes*. *Industrial & Engineering Chemistry Research*, 2013. **52**(3): p. 1122-1132.
89. Hayashi, J.-i., et al., *Effect of Oxidation on Gas Permeation of Carbon Molecular Sieving Membranes Based on BPDA-pp'ODA Polyimide*. *Industrial & Engineering Chemistry Research*, 1997. **36**(6): p. 2134-2140.
90. Kusakabe, K., M. Yamamoto, and S. Morooka, *Gas permeation and micropore structure of carbon molecular sieving membranes modified by oxidation*. *Journal of Membrane Science*, 1998. **149**(1): p. 59-67.
91. Hayashi, J.-i., et al., *Pore size control of carbonized BPDA-pp' ODA polyimide membrane by chemical vapor deposition of carbon*. *Journal of Membrane Science*, 1997. **124**(2): p. 243-251.

92. Salleh, W.N.W., et al., *Precursor Selection and Process Conditions in the Preparation of Carbon Membrane for Gas Separation: A Review*. Separation & Purification Reviews, 2011. **40**(4): p. 261-311.
93. Dutczak, S.M., et al., *New crosslinking method of polyamide–imide membranes for potential application in harsh polar aprotic solvents*. Separation and Purification Technology, 2013. **102**: p. 142-146.
94. Wallace, D.W., et al., *Characterization of crosslinked hollow fiber membranes*. Polymer, 2006. **47**(4): p. 1207-1216.
95. Nishino, T., et al., *Residual stress and microstructures of aromatic polyimide with different imidization processes*. Polymer, 2000. **41**(18): p. 6913-6918.
96. Dygert, N.L., et al., *Deposition of polyimide precursor by resonant infrared laser ablation*. Applied Physics A, 2007. **89**(2): p. 481-487.
97. Chen, S.A. and H.T. Lee, *Polyaniline plasticized with 1-methyl-2-pyrrolidone: structure and doping behavior*. Macromolecules, 1993. **26**(13): p. 3254-3261.
98. Ebisawa, S., et al., *Spontaneous molecular orientation of polyimides induced by thermal imidization (5). Effect of ordered structure formation in polyimide precursors on CTE*. European Polymer Journal, 2010. **46**(2): p. 283-297.
99. Chang, K.-S., et al., *Residual Solvent Effects on Free Volume and Performance of Fluorinated Polyimide Membranes: A Molecular Simulation Study*. The Journal of Physical Chemistry B, 2009. **113**(30): p. 10159-10169.

100. Fu, Y.-J., et al., *Effects of residual solvent on gas separation properties of polyimide membranes*. Separation and Purification Technology, 2008. **62**(1): p. 175-182.
101. Weng, T.-H., H.-H. Tseng, and M.-Y. Wey, *Effect of SBA-15 texture on the gas separation characteristics of SBA-15/polymer multilayer mixed matrix membrane*. Journal of Membrane Science, 2011. **369**(1–2): p. 550-559.
102. Rutherford, S.W. and D.D. Do, *Review of time lag permeation technique as a method for characterisation of porous media and membranes*. Adsorption, 1997. **3**(4): p. 283-312.
103. Nik, O.G., X.Y. Chen, and S. Kaliaguine, *Amine-functionalized zeolite FAU/EMT-polyimide mixed matrix membranes for CO<sub>2</sub>/CH<sub>4</sub> separation*. Journal of Membrane Science, 2011. **379**(1–2): p. 468-478.
104. Nik, O.G., X.Y. Chen, and S. Kaliaguine, *Functionalized metal organic framework-polyimide mixed matrix membranes for CO<sub>2</sub>/CH<sub>4</sub> separation*. Journal of Membrane Science, 2012. **413–414**(0): p. 48-61.
105. Alexander Stern, S., *Polymers for gas separations: the next decade*. Journal of Membrane Science, 1994. **94**(1): p. 1-65.
106. Mahajan, R. and W.J. Koros, *Factors Controlling Successful Formation of Mixed-Matrix Gas Separation Materials*. Industrial & Engineering Chemistry Research, 2000. **39**(8): p. 2692-2696.
107. Grisdale, R.O., *The Properties of Carbon Contacts*. Journal of Applied Physics, 1953. **24**(10): p. 1288-1296.

108. Laine, N.R., F.J. Vastola, and P.L. Walker, *THE IMPORTANCE OF ACTIVE SURFACE AREA IN THE CARBON-OXYGEN REACTION*<sup>1,2</sup>. The Journal of Physical Chemistry, 1963. **67**(10): p. 2030-2034.
109. Kinoshita, K., *Carbon: electrochemical and physicochemical properties*. 1988.
110. Yamamoto, M., et al., *Carbon molecular sieve membrane formed by oxidative carbonization of a copolyimide film coated on a porous support tube*. Journal of Membrane Science, 1997. **133**(2): p. 195-205.
111. Schindler, E. and F. Maier, *Manufacture of porous carbon membranes*. 1990, Google Patents.
112. He, X., et al., *Preparation and Characterization of Hollow Fiber Carbon Membranes from Cellulose Acetate Precursors*. Industrial & Engineering Chemistry Research, 2011. **50**(4): p. 2080-2087.
113. Kaburagi, Y. and Y. Hishiyama, *Ferromagnetism discovered on heat-treating the aromatic polyimide film Kapton*. Journal of Materials Research, 2002. **17**(08): p. 2000-2006.
114. Su, J. and A.C. Lua, *Effects of carbonisation atmosphere on the structural characteristics and transport properties of carbon membranes prepared from Kapton® polyimide*. Journal of Membrane Science, 2007. **305**(1–2): p. 263-270.
115. <http://periodictable.com/Elements/006/data.html>
116. Lee, P.-S., et al., *Carbon molecular sieve membranes on porous composite tubular supports for high performance gas separations*. Microporous and Mesoporous Materials, 2016. **224**: p. 332-338.

117. Vu, D.Q., W.J. Koros, and S.J. Miller, *Mixed matrix membranes using carbon molecular sieves: I. Preparation and experimental results*. Journal of Membrane Science, 2003. **211**(2): p. 311-334.
118. Yoshimune, M. and K. Haraya, *CO<sub>2</sub>/CH<sub>4</sub> Mixed Gas Separation Using Carbon Hollow Fiber Membranes*. Energy Procedia, 2013. **37**: p. 1109-1116.

## **ACKNOWLEDGEMENTS**

This study has been supported by King Abdulaziz City for Science and Technology through the projects # 11-32-أت and TIC-CCS-5.

## Vitae

Name :Tanveerulla Hussain Syed

Nationality :Indian

Date of Birth :8/18/1990

Email :syed.care4u@gmail.com

Address :KFUPM

Academic Background :M.S in Mechanical Engineering

Status of Publication

1. Tanveerulla Hussain Syed, Khaled Mezghani\*, Sarfaraz Furquan, Enhancing the Permeation Properties of Carbon Molecular Sieve for O<sub>2</sub>/N<sub>2</sub> Separation Using Thermal and Chemical Treatments, 2016 (to be submitted).